University of Rome "Tor Vergata"

Institute CNR-TAE

University of Rome "Tor Vergata"

Ph.D. course in "*Materials for Environment and Energy*"

(Cycle XXI)

Investigation on low and high temperature fuel cell components and their evaluation in short stack configuration

Giovanni Brunaccini

A.A.: 2008/2009

Supervisor:

Dr. Antonino Aricò

Director:

Prof. Silvia Licoccia

Index

Abstract

Research activities on solid oxide (SOFC) or polymer electrolyte membrane (PEMFC) fuel cells are currently focused on performance and lifetime enhancement as well as costs reduction. These aspects are relevant to make such systems more attractive for the market, both for stationary and automotive applications.

From this point of view, an increase of temperature (for 80°C to 110-120°C) appears necessary for PEMFC technology (high temperature PEMFC, or HT-PEMFC). This would allow more resistance to CO contaminants in the fuel, better thermal and water management and a better efficiency for co-generation.

On the contrary, SOFC technology is moving towards intermediate temperature (IT-SOFC); this would allow cost reduction while developing planar cells, due to less critical construction processes and an increase of stability.

These ways to enhance the fuel cells applications are well studied for single cell but the scale-up process to significant power production devices needs specific investigations. Moreover, different technologies need different field test procedures, tailored on the specific application sectors.

In this Ph.D. thesis, fuel cell devices exploiting either solid oxide or polymer electrolyte technologies, were tested for specific applications. In particular, 1kW fuel cell stacks were tested in order to verify the possibility of fuel cell use in small size applications.

Nowadays, HT-PEMFC devices are creating lot of interest for FC technology development. Anyway, despite a deep knowledge of material properties, the assessment of the new materials at stack level have undergone only few studies. In this research activity this aspect was investigated.

Moreover, IT-SOFC technology is considered valuable for stationary applications and distributed energy production, using cheap fuels and a highly efficient electrochemical process. Nevertheless, for residential energy

consumption, the studied SOFC device can be considered not as a downscaled device for laboratory study, but as the base to develop a complete system.

This Ph.D. thesis involves considerations for both stationary and automotive applications, by analysing fuel cells stack with a size large enough to be considered a proof-of-concept. In other words, the size appears sufficient to investigate main phenomena visible in larger stack oriented to real world applications.

The whole activity can be divided in two lines:

1) tests of HT-PEMFC short stacks that were carried out to evaluate their performance in typical automotive working conditions (current, temperature, humidification, pressure) and to establish an optimal operating point.

2) tests of IT-SOFC stacks in natural gas, in order to evaluate performance decay and its response to detrimental effects due to thermal and redox cycles that can appear in "out of laboratory" usage.

Diagnostic analysis such as current interrupt method and electrochemical impedance spectroscopy completed the study by supplying information about the optimization of stack assembling procedure.

The whole experimental activities were carried out in laboratory, to accurately control the process variables; nevertheless, the recorded performances are anyway meaningful with respect to real world applications, once defined tailored working conditions by a good compromise between performances and costs.

Introduction

Background

Sustainable energy sources are now attracting great interest, mainly due to the aspects related to environment protection and energy saving. Among the various energy conversion technologies, Fuel Cells (FCs) seem to be effective conversion devices thanks to their high efficiency electrochemical processes, which are independent on the Carnot thermodynamic efficiency limitation, with respect to internal combustion engines [1]. Among the FCs, two technologies are considered particularly interesting for small size applications, the Polymer Electrolyte Membrane Fuel Cells (PEMFCs) and the Solid Oxide Fuel Cells (SOFCs). These two technologies work in very different temperature ranges (typically 40 to 90°C for PEMFCs and 800 to 1000°C for SOFCs), fed with different fuels, and with different needs for working condition control apparatus. These technologies show different advantages and drawbacks and, as a consequence, they must be tailored to be suitable for different fields of applications.

The main physical and working parameters can be summarised as follows in **Table 1**:

Fuel Cell Technology	PEMFC	SOFC
Electrolyte material	Polymer	Ceramic
Catalyst	Pt based	Ni based
Anode fuels	Hydrogen	Hydrogen, hydrogen-CO mixtures, low-weight hydrocarbons, natural gas (desulphured)
Poisoning fuel impurities	CO, Sulphur	Sulphur
Typical temperature range	40 – 90°C	800 – 1000°C
Start-up time	< 1min	Few hours
Sensitivity to thermal cycles	Devices can be switched on and off several times	Only few thermal cycles can be imposed
Power density	450 – 500 mW/cm^2	300 – 350 mW/cm^2

Table 1: Physical and electrochemical parameters to describe working conditions for PEMFCs and SOFCs

With reference to the fuels used to feed these kind of cells, SOFC devices offer the possibility of internal gas reforming. Reforming reactions convert the mixture flowing at the system gas inlet in a hydrogen rich stream, capable of supplying the stack with only minimum carbon deposition probability. This process (that, if needed, is done in external reactors for PEMFCs) reduces the overall size (and cost) of turnkey systems. On the contrary, strict requirements include the necessity of full removal of sulphur and sulfated compounds, because, according to the state-of-the-art technology, even a small content of these substances damage the cells and reduce the device lifetime [2].

In order to convert the intrinsic potential of fuel cell devices in market attractive turn-key systems, the above mentioned drawbacks must be mitigated.

One of the possible ways to reduce costs and technical problems to put these devices in the market is the extension of their operative temperature range, this action would bring appreciable advantages for both considered technologies. This

procedure leads to the study of so-called Intermediate Temperature SOFCS (or IT-SOFCs) [3] and High Temperature PEMFCs (or HT-PEMFCs) [4].

Advantages of temperature reduction for SOFCs operation

Concerning with SOFCs, high operation temperatures lead to the use of high quality and expensive steel for the fabrication process of stack plates, due to the need of avoiding plates oxidation during operation. For commercial viability of a small size SOFC devices in residential applications, the stack contribution to the total cost is usually considered about 30% of the complete system. In order to achieve such a target, the degradation rate of the device's components needs to be taken into account. For this reason, decreasing operating temperature helps to satisfy market requirements, by allowing for a replacement of traditional oxidation resistant alloys with cheaper ferritic stainless steels. This replacement is valid both for plates and current collectors. Secondly, planar technology is expected to reduce costs by using a simplified construction process like tape casting of the cells [5].

Moreover, high temperature implies higher energy requirement during the start-up phase, by using more power to bring the stack at the right temperature and a more expensive insulation chamber in order to maintain temperature and to avoid electromagnetic interference (from thermal irradiance) on the control system. Finally, the higher is temperature the higher is the mechanical stress at the electrode/electrolyte interface (due to the different volume variation coefficient for different materials), especially for large planar cells that are considered well promising for cost reduction in a mass market.

For these reasons, a diminution of the operating temperature is a first step to make this kind of device more attractive for the market, because higher electrochemical stability of materials assures longer lifetime of the devices.

On the other hand, high temperature allows the utilization of cheap electrocatalysts (like nickel that shows good catalytic activity for H_2 and CH_4 oxidation at 750°C) and ceramic electrolytes (that become conductive for O^{2-} ions

only at high temperature); so, while operating at lower temperature, it is necessary to assess the performance of the device under test.

In this thesis work, both new SOFC materials and stack devices were tested under different conditions.

Needs for increasing operation temperature in PEMFCs

Similarly to SOFC systems, a higher temperature range is desirable for PEMFCs for different reasons.

Firstly, for cogeneration applications, the heat produced at high temperature is characterised by higher exergy content [5]. The heat transfer is, in fact, proportional to the temperature gradient from the source (the fuel cell) to the drain (the external plant).

The effect on the overall cost reduction is due to the higher reachable efficiency; in fact, the electrochemical reaction of H_2 oxidation for electrical power production is exothermal and the hot water produced at the cathode of the stack can be used in a heat exchanger to improve the conversion efficiency (from fuel to electrical power and heat) of the cell.

Moreover, at higher temperature, PEMFC stacks show a better resistance to contaminants in the fuel [6]; in fact, CO content (due to the no ideal operation of the hydrocarbons reforming systems) in H_2 causes deactivation of the anode catalyst in the long run. This phenomenon happens because the typical catalyst for PEM fuel cells is platinum; Pt atoms adsorb CO and, as a consequence, the number of active sites to allow the adsorption of H_2 decreases, affecting the cell performance.

The adsorption process of CO on Pt is more significant at low temperature (about 80°C) and decreases at higher temperature [7]. In particular, moving from 80°C to 130°C, the tolerance to CO presence in a PEM stack grows from 10 to 1000ppm. This feature allows for the utilization of H_2 produced by means of a reformer without any extra purification methods and with significant cost reduction in out-of-laboratory applications.

At low temperature, the poisoning effect can be made milder if O_2 is added in the fuel stream or if advanced catalysts (resistant to CO poisoning) are used. Anyway, the former action causes fuel utilization reduction, the latter obligates to use experimental materials not available in commercial device in short term.

From the kinetic point of view, high temperature positively affects the reversible potential and the slope of the Tafel equation, but it has negative effect on the OCV value.

In general, the reversible potential variation due to a temperature variation is described by the Nernst equation:

$$\frac{\partial E_{rev}}{\partial T} = \frac{\Delta S}{nF}$$

at a given constant pressure. For a fuel cell fed with hydrogen and air, the right-hand side of this equation is strongly negative below 100°C; on the contrary, above 100°C the produced water is present as steam, and the entropy variation is lower.

In contrast over 100°C, OCV value, that includes the voltage drop due to activation effects, is lowered by the increased value of the H_2O pressure in the expression:

$$OCV = E_{rev} + \frac{RT}{2F}\ln\left(\frac{p_{H_2} * p_{O_2}}{p_{H_2O}}\right).$$

Another temperature effect on the Tafel equation is the increment of the exchange current density (i_o) from low to higher temperatures for Nafion based membranes [9], about 30 times for a 40°C temperature increment.

Furthermore, while a PEMFC device is working at a temperature over 100°C, the risk of flooding phenomena is reduced thanks to the water evaporation; on the contrary, the dehydration could increase due to the heat production and, as a consequence, the proton conductivity of the membrane decreases. A dramatic decrease of the conductivity is typically experienced below 30% R.H.

Secondly, in the long term, deep variations of water content may lead to mechanical stress of the membrane, due to subsequent swelling and shrinking phenomena.

For commercial applications (for which PEMFCs are still too expensive [10]), the cost reduction comes also with the presence of cheaper and simpler thermal management systems. From this point of view, the heat produced by the electrochemical reaction and the Joule effect in the device, is as more easily moved away from the cells as higher is the temperature gradient toward the ambient temperature. Hence, at higher temperature, a higher amount of heat is moved away and a less severe control on the thermal management can be implemented, with a consequent size and cost reduction for the cooling system.

High temperature issues for PEMFC devices

Despite the above described enhancement achieved by increasing temperature, some critical factors must be considered. As the proton conductivity of the membrane is reduced at low relative humidity, the evaporation of water content into the membrane lead to a major issue when cells operates over 100°C [11]. In practical applications, commonly used Nafion membranes show dehydration when operated at temperature over 90°C.

Moreover, the thermal management system must control the temperature distribution within the device. In particular, high temperature can cause the creation of hot spots on the membrane, leading to extra mechanical stress or local dehydration with subsequent deformation and damage. This causes a reduced lifetime of the devices and increasing costs.

Moreover, the effect of possible degradation of components into the device must be assessed during high temperature operations. The degradation of a single component (catalyst, catalyst support, electrode) affects the overall performance of the device and the related lifetime. Typical degradation can be attributed to catalyst support corrosion (that reduces catalyst stability) and to catalyst dissolution.

Description of the developed activities

Concerning with IT-SOFCs, two 1kW commercial stacks were characterised in H_2 and in (desulfurized) natural gas (NG), in order to evaluate the performance

characteristics and to identify the main problems related to the scale-up process. Materials investigation was carried out at the level of cell. According to the state-of-the-art and commercial forecast, planar cell technology was selected.

The tests, carried out under different conditions, allow to derive useful information for the selection of auxiliary devices during the engineering process while developing a complete SOFC power generation system around the stack.

The aim is to assess SOFC performance both in H_2 and NG (mainly CH_4). Obviously, better results are expected in H_2 than in NG; anyway, natural gas, that unlike hydrogen is already available to residential users without any modification of the current gas distribution infrastructure, can be directly fed into SOFC devices that operate in the internal reformation mode.

Hence, for the short/mid term exploitation, NG performance are more important for mass market distribution, and H_2 is to be considered as an ideal target for the tested technology. Moreover, exhaust gas emissions can be recycled in advanced applications using them as heating input for absorption heating and cooling systems.

The second part of this work deals with HT-PEMFCs, a 1kW short stack (6 cells) was tested under automotive relevant conditions. A wide range of temperatures was investigated (from 30°C to 130°C) and pressure as well, in order to find optimal operating conditions. Moreover, the assembling process was optimised. Diagnostics was performed by Current Interrupt Method (CIM), Electrochemical Impedance Spectroscopy (EIS) and hydrogen crossover tests. Relationships between stack components characteristics and electrochemical behaviour were investigated.

References

[1] Kunze, J; Stimming, U. - Angewandte Chemie International Edition Volume: 48, Issue: 49, November 23, 2009, pp. 9230-9237

[2] Nyqvist, R.G.; de Bruijn, F.A.; Stobbe, E.R. - Journal of Power Sources Volume: 159, Issue: 2, September 22, 2006, pp. 995-1004 de Wild, P.J.;

[3] Huijsmans, J.P.P.; van Berkel, F.P.F.; Christie, G.M. - Journal of Power Sources Volume: 71, Issue: 1-2, March 15, 1998, pp. 107-110;

[4] Mallant, Ronald K.A.M. - Journal of Power Sources Volume: 118, Issue: 1-2, May 25, 2003, pp. 424-429

[5] Saidi, M.H.; Ehyaei, M.A.; Abbasi, A. - Journal of Power Sources Volume: 143, Issue: 1-2, April 27, 2005, pp. 179-184

[6] Scott, K.; Shukla A.K.; Reviews in Environmental Science & Bio/Technology (2004) 3:273-280

[7] Zhang, Jianlu; Xie, Zhong; Zhang, Jiujun; Tang, Yanghua; Song, Chaojie; Navessin, Titichai; Shi, Zhiqing; et. al. - Journal of Power Sources Volume: 160, Issue: 2, October 6, 2006, pp. 872-891

[8] Das, Susanta K.; Reis, Antonio; Berry, K.J.;Journal of Power Sources Volume: 193, Issue: 2, September 5, 2009, pp. 691-698

[9] Parthasarathy et al. - J of electr.soc. – 1992

[10] Scholta, J.; Berg, N.; Wilde, P.; Jörissen, L.; Garche, J.; Journal of Power Sources 127 (2004) 206–212

[11]Licoccia, S.; Traversa, E.; Journal of Power Sources Volume: 159 (2006), pp. 12-20.

Chapter 1

Experimental characterization of IT-SOFC in single cell and stack configuration with different fuels

1.1 - Characterization of innovative single cell based on Ni-doped Perovskite anode catalyst

1.1.1 - Introduction

The direct oxidation of hydrogen and hydrocarbons in intermediate temperature solid oxide fuel cells (IT-SOFCs) has been intensively investigated due to the high intrinsic efficiency of the direct electrochemical oxidation process.

A significant attention has been focused on hydrogen and methane electro-oxidation by using electrocatalysts such as Cu/CeO_2, Ni-Cu and various perovskites [1, 2]. Encouraging results have been achieved at temperatures below 800°C, especially in the presence of ceria electrolyte.

Some attempts have been addressed to the direct oxidation of hydrogen and larger molecular weight hydrocarbons [1]. It has been observed that the kinetics of direct electrochemical oxidation of propane is slower than methane and, moreover, it is more affected by the cracking process producing carbon fibres on the anode surface, especially in the case of Ni-based catalysts. The formation of carbon deposits also occurs under steam reforming conditions at intermediate temperatures. Accordingly, it appears necessary to investigate alternative catalysts for both direct electro-oxidation and steam reforming of propane in IT-SOFCs.

Recently, several investigations have been addressed to the use of Ru as promoter of anodic processes in SOFCs [3-4]. Yet, the high cost of Ru suggests searching for an alternative catalyst formulation with similar activity at intermediate temperatures.

In this work, efforts were focused on the investigation of the effect of Ni in combination with $La_{0.6}Sr_{0.4}Fe_{0.8}Co_{0.2}O_3$ and ceria (Ni-LSFCO/CGO) as oxidation catalyst for propane in intermediate temperature SOFCs.

In order to evaluate the characteristics of this catalytic system propane direct electro-oxidation process has been evaluated in a ceria-electrolyte supported single cell.

1.1.2 - Experimental

Based on a Ni-LSFCO/CGO anode catalyst, a button cell, whose area is $1cm^2$, was prepared at CNR-ITAE.

It consisted of 3 layers listed in **Table1.1**:

Layer	Composition	Thickness [µm]
Anode	Ni-LSFCO 70% CGO 30%	15
Electrolyte	CGO	250
Cathode	LSFCO/CGO	15

Table 1.1: Cell components description. Noticeable are the Ni-LSFCO used as anode catalyst and a 250µm thick electrolyte layer

After mounting the cell on an alumina tube, it was heated up to 800°C in He stream. At 800°C, the gas was switched to H_2 and suddenly as the potential reached the OCV it was switched to 500 mV preventing an extensive reduction of perovskite. Subsequently, the anode was fed with dry propane under working condition at 500 mV. It is inferred that during its operation in the SOFC, the Ni-LSFCO anode is not subjected to strong reducing conditions for prolonged times. The reducing environment at the anode is mitigated by both the cell potential fixed at 500 mV and the mixed electronic/ionic conduction of CGO electrolyte that does not allow it to reach high OCV associated with a very low oxygen partial pressure at the anode. Electrochemical polarizations and ac-impedance measurements were performed on electrolyte supported single cells at 800°C by using an AUTOLAB PGSTAT30 Metrohm potentiostatic frequency-response analyzer equipped with 20A booster. Gold wires were used as current collectors

for the cell. A thermocouple was positioned close to the cell. Impedance spectra were obtained in the frequency range from 10 mHz to 1 MHz with applied ac-voltage amplitude of 10 mV rms. All impedance measurements were taken under open circuit conditions and 500 mV.

Although LSFCO perovskite is not stable in the presence of methane (in out-of-cell measurements), it improves its stability during SOFC operation in a CGO based cell due to the mild anodic reducing conditions [5]. It is pointed out that the strong reducing conditions in the presence of hydrocarbons in the out of cell experiment are significantly alleviated during SOFC operation thanks to oxygen pumping effect from the cathode to the anode. AC impedance analysis of the SOFC cell operating in the presence of H_2 in the range 700-800°C, reported in **Figure1.1**, under working conditions (500 mV) shows appropriate polarization resistances essentially above 700°C. The Rs decreases from 0.43 Ω·cm^2 at 700°C to 0.25 Ω·cm^2 at 800°C. These ohmic losses are due to the supporting 250 µm membrane electrolyte. Polarization resistance is lower than 0.3 Ω·cm^2 at 750°C.

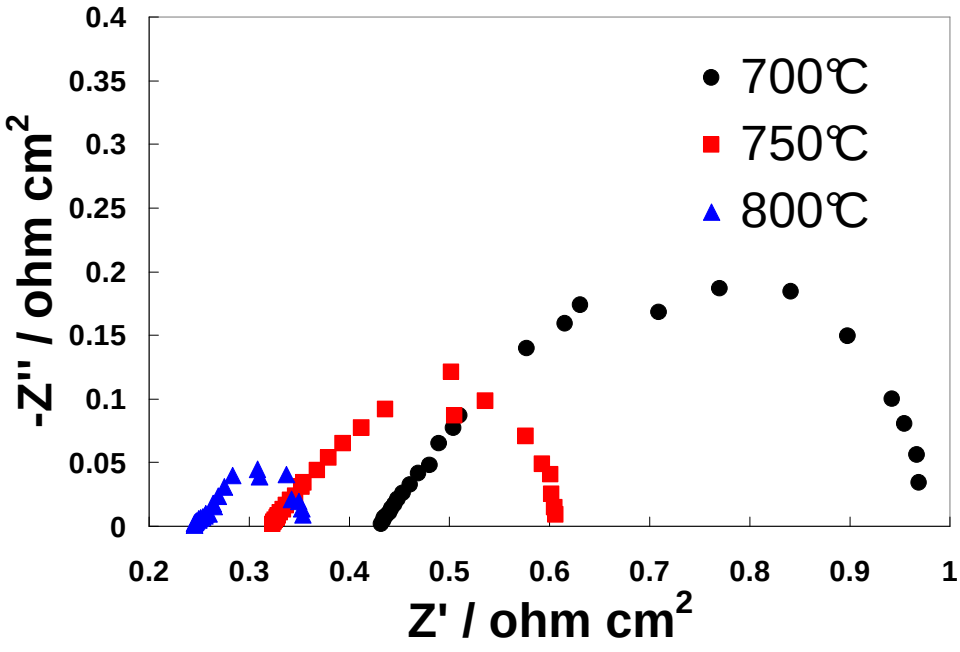

Figure 1.1: AC impedance analysis of the SOFC cell operating in presence of H_2 between 700°C-800°C under working conditions (500mV), shows appropriate polarization resistances essentially above 700°C. The Rs decrease from 0.43 Ω·cm$_2$ at 700°C to 0.25 Ω·cm2 at 800°C. Polarization resistance is lower than 0.3 Ω·cm$_2$ at 750°C.

In **Figure 1.2**, polarization curves carried out in H_2 show that the maximum power density increases with temperature (421 mW·cm^{-2} at 800°C) whereas the OCV decreases due to the electronic conduction of CGO [6].

The performance of perovskite anodes in the presence of methane feed has been previously investigated [5]. In the present work, the attention is addressed to operation of the anode with propane. Impedance spectra were carried out at 800°C after different operating times of the cell in the presence of dry propane at open circuit voltage conditions. **Figure 1.3** shows that the initial resistance in propane is larger than in H_2 (0.32 vs. 0.25 Ω·cm^2). Possibly, after the switch to H_2, the electrode is partially reoxidized due to a decrease in reducing conditions. During operation, the increasing depth of the reduction process and possibly a small amount of carbon deposition on the catalyst causes decrease of both ohmic and polarization resistances practically achieving the same results obtained in hydrogen, i.e. Rs= 0.25 Ω·cm^2 and Rp=0.07 Ω·cm^2 at 800°C. The observed R_p value in propane at 800°C (0.10 Ω·cm^2 at 0 hrs and 0.07 Ω·cm^2 after 101 hrs), indicate suitable reaction rates.

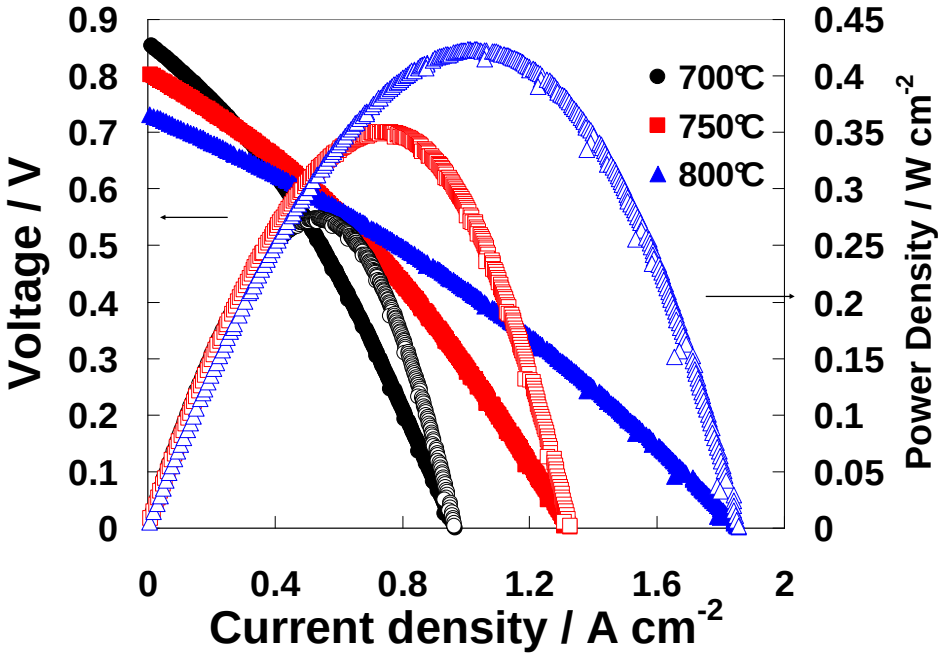

Figure 1.2: Polarization curves carried out in H_2 show that the maximum power density increases with temperature (421 mW·cm^{-2} at 800°C) whereas the OCV decreases due to the electronic conduction of CGO.

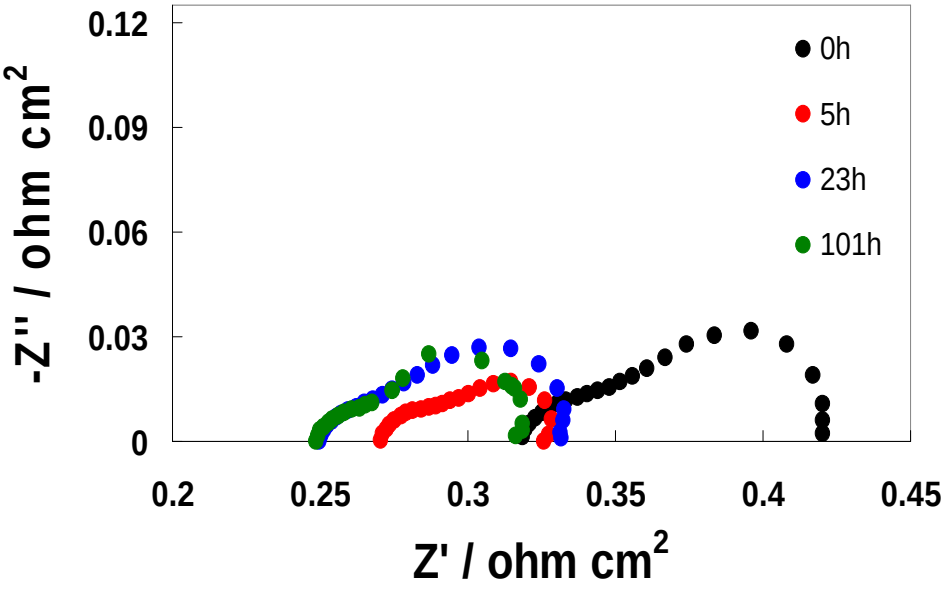

Figure 1.3: AC impedance analysis of the SOFC cell operating shows initial resistance in propane is higher than in H_2 (0.32 vs. 0.25 Ω·cm²). After operation it become comparable to the one observed in H_2, i.e. Rs= 0.25 Ω·cm² and Rp=0.07 Ω·cm² at 800°C. The observed Rp values in propane at 800°C (0.10 Ω·cm² at 0 hrs and 0.07 Ω·cm² after 101 hrs) indicate suitable reaction rates.

Figure 1.4 shows polarization curves in dry propane feed at 800°C after different operating times of the cell. A maximum power density of about 300 mW/cm² was obtained after 101 h of lifetime. Both polarization and impedance spectra indicate that the direct electro-oxidation of propane can be suitably performed in the temperature range of 800°C. The output power density of the present device (300 mW·cm^{-2} at 800°C) is mainly affected by ohmic drop and low OCV, essentially related to the electrolyte membrane thickness and electronic conduction than to the catalyst properties.

No evident carbon deposits or tar formation was observed on the anode surface after cell shut down. Some amount of carbon was present in the wall of the alumina tube and a pitchy fluid apparently came out from the anode compartment during cell operation.

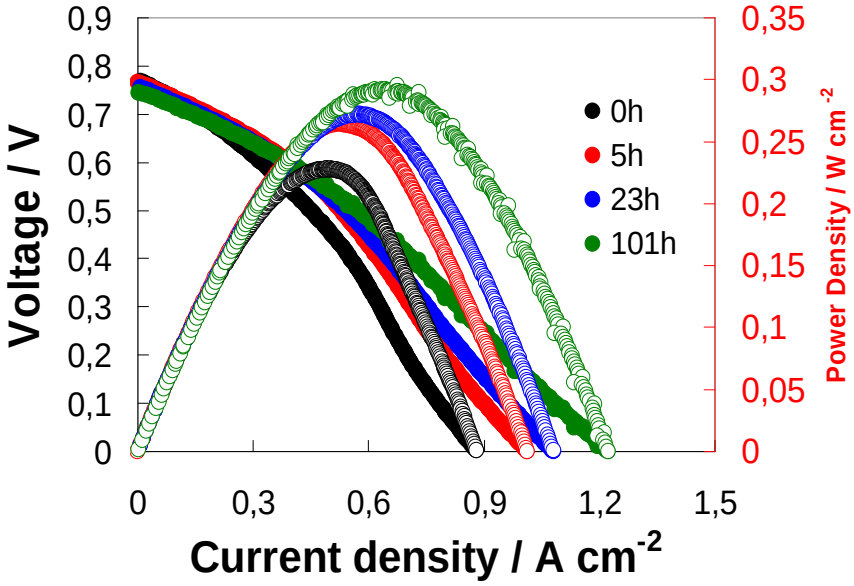

Figure 1.4. Polarization curves at different times in propane at 800°C. Both polarization and impedance spectra indicate that the direct electro-oxidation of propane can be suitably performed in the temperature range of 800°C. The output power density of the present device (300 mW cm^{-2} at 800°C) is mainly affected by ohmic drop and low OCV, essentially related to the electrolyte membrane thickness and electronic conduction than to the catalyst properties.

Clearly, the performance of the present SOFC may be greatly enhanced if a thin electrolyte is used (reducing ohmic drop) and if the CGO electrolyte membrane is replaced by another electrolyte characterized by a higher ionic transport number under such conditions. In fact, high ohmic drop and low OCV affect the performance of the present SOFC device. Whereas, the polarization resistances in dry propane were quite promising and indicate that this catalyst can properly operate without the need to use noble metals like Ru, Rh, etc. to promote the oxidation process. As well known Ni promotes the C-H bond scission and thus, the direct oxidation but, during hydrocarbons operation, it also significantly increases the probability of irreversible deposition of carbon species at the surface blocking the catalytic sites with time.

Breaking of the carbon-hydrogen bond is considered to be the activation step in the direct oxidation process [8] followed by removal of the adsorbed species by O^{2-} ions. Long term operation of Ni under dry operation is questioned, as discussed above, due to the growth of carbon deposits. On the other hand, CGO

has been identified as a suitable oxidation catalyst for both H_2 and methane [9]. The rate determining step on this oxide catalyst presently appears to be related with the scission of C-H bond the combination of highly dispersed Ni with a highly electronic/ionic conductor such as LSFCO perovskite, significantly reduces the carbon deposition under mild anode reducing condition in the presence of CGO.

1.1.3 – Conclusions

Direct oxidation of hydrogen and propane on a Ni-LSFCO/CGO electro-catalyst has been investigated at intermediate temperatures (800°C) in a CGO electrolyte supported cell [10]. The measured electrochemical performances were affected by low OCV, whereas interesting polarization resistances were recorded.

No carbon deposit was observed in the catalyst discharged after operation of the anode under mild reducing condition in a SOFC. The achieved performance for hydrogen and propane oxidation are both acceptable even in the presence of a thick electrolyte membrane. However, the electric efficiency is still not appropriate (the maximum power density is achieved at about 500 mV). It is envisaged that an increase of electric efficiency may be achieved by improving the reversibility of the process (i.e. decreasing the polarization resistance) and reducing the ohmic resistance while maintaining mild reducing conditions at the anode that are essential to preserve the perovskite structure.

1.2 - Steam reforming based 1kW planar SOFC stack

1.2.1 - Introduction

Based on the results of studied materials, an intermediate temperature SOFC stack was built and tested, in order to evaluate the reachable performance when a scale up is applied to the button cells. Moreover, the characterization of stacks is an intermediate step to the prototype production of a turn-key fuel cell system.

From this point of view, a 75 solid oxide fuel cell stack was tested both in hydrogen and in methane from natural gas. The work is intended to give a high

repeatability stack study with particular attention to power performance in different operating conditions in order to extend stack life time. The achieved stack power was higher than 1 kW in hydrogen and about 0.98 kW in natural gas.

An accurate conditioning procedure was accomplished in order to avoid cracks in the cells, electrode delamination and anode catalyst reoxidation. A few thermal cycles were performed. This study allowed to evaluate the performance and efficiency of planar SOFC cells based stack. The time study indicated proper stability for the device operation even in the presence of thermal cycles.

1.2.2 - Hardware description

The tested stack (visible in **Figure 1.5a**) was composed of 75 SOFC planar (9.6x9.6 cm^2) cells and was equipped with 8 voltage probes to sample the voltage of 7 groups of cells.

In particular, the first two, the central cell (cell #38), and the last two cells were individually monitored, in addition the remaining ones were sampled as two 35-cell substacks each.

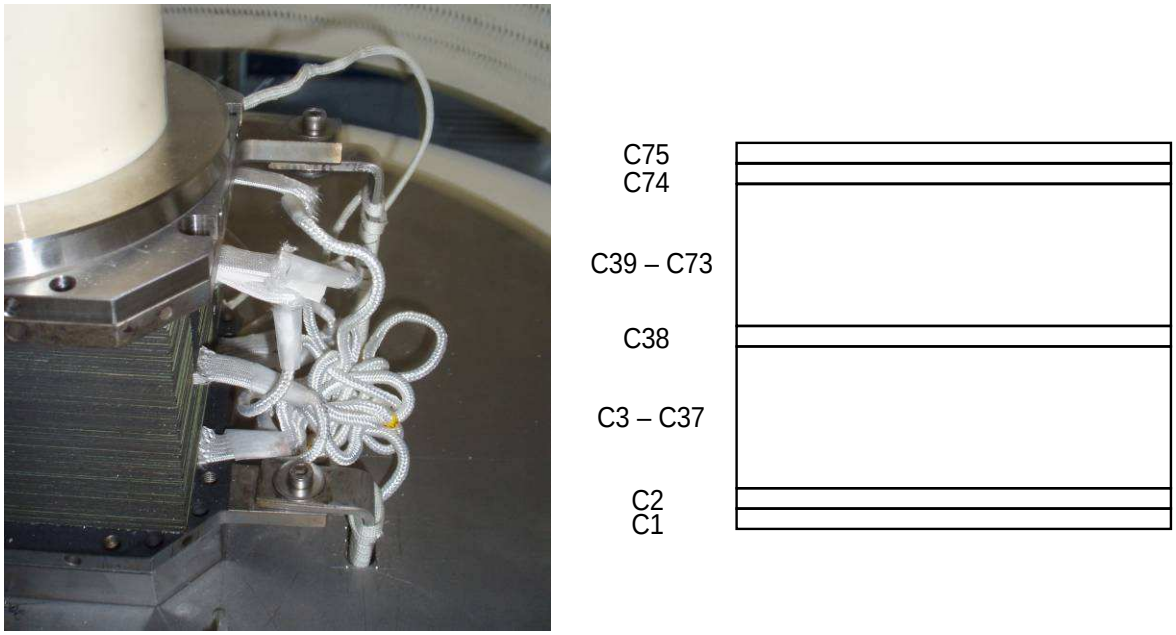

Figure 1.5: (a) 1kW SOFC stack tested in this work - (b) sketch of the voltage probes distribution to sample single cell and substack voltages

The test bench (shown in **Figure 1.6**) was equipped with specific hardware to control stack temperature, gas flows and to apply a variable electric load.

Particular attention was paid to guarantee complete insulation of the current collectors of the stack from each other and from the test bench chassis; to achieve this condition, the insulation of the power input terminals of the electronic load were checked.

High temperature insulating gaskets were used to separate the cathode compartment from the test bench chassis ground to avoid short circuit effects that would have brought the single cells operating point too low, i.e. under conditions where Ni easily reoxidizes at the anode. On the other hand, the anode electrode was separated from the chassis ground by a long alumina cylinder, this is because the upper side of the stack undergoes the pressure of the mechanical load to maintain the cells in row tightly close each other without any leakage.

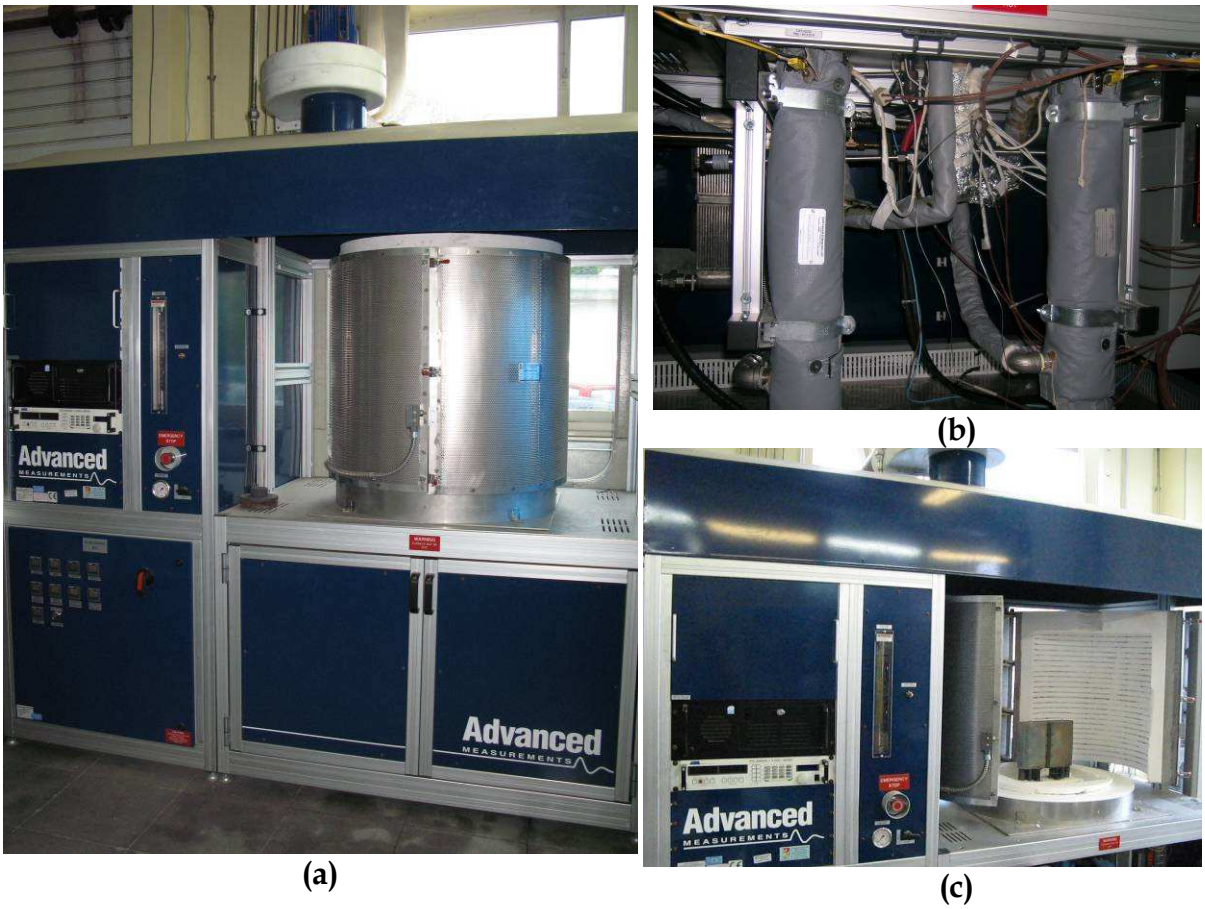

Figure 1.6: The used test rig (a) and a close-up on gas pre-heaters (b) and electrical furnace (c)

Due to the high pressure of the mechanical load, in order to avoid strains and bending of the steel slab supporting the furnace basement, the system was provided with a pair of rigid steel wired rods to finely regulate a counter pressure.

Moreover, to deal with natural gas, the plant was equipped with a pre-reformer to convert hydrocarbons heavier than methane (e.g. propane) that can poison the anode catalyst by forming carbon deposits.

Natural gas was fed by pre-reforming it in a dedicated catalytic converter operating in the range 350 - 450 °C. The output gas flow was regulated (at the input of test bench) with a mass flow calibrated as for CH_4; according to the gas analysis, it was determined that the most part of the feeding gas was methane.

The gas mixture coming from the pre-reformer was supplied to the anode compartment thanks to the internal reforming occurring into the stack. This process enriched the hydrogen content of the mixture by converting the CH_4 in H_2 and CO_2 through the reaction of steam reforming and possibly a subsequent water gas shift [11]:

$$CH_4 + H_2O \rightleftharpoons CO + 3H_2$$

$$CO + H_2O \rightleftharpoons CO_2 + H_2.$$

Thus, for each mole of CH_4 in the natural gas stream, 4 moles of H_2 are obtained.

In the whole process, steam reforming reaction is strongly endothermic, whereas water gas shift reaction is exothermic. Thus, a part of heat required was provided by the latter reaction, and lower electrical heating power was required while feeding the cathode compartment with air. Moreover, steam reforming is characterised by a minor sensitivity to thermodynamic conditions (with respect to dry reforming) for carbon formation, thanks to the higher hydrogen/carbon ratio, and converts natural gas in a mixture with quite high hydrogen concentration. Anyway, for turnkey systems, the necessity of finely regulate the steam content of anode stream leads to higher costs and control hardware complexity.

During the laboratory tests, a humidifier was used to add the correct amount of water steam, and a steam-to-carbon ratio (S/C) always larger than 2 was imposed. As described later, different values were attempted, in order to find a compromise between voltage stability and performance.

The test stand was equipped with a humidifying device containing deionized water, that, in turn, (by evaporation) provide the gas with a saturating amount of

steam, according to the desired steam/carbon ratio. The temperature of deionized water was automatically regulated and, to avoid the presence of liquid droplets in gas stream, the steam was accordingly introduced only when the correct temperature was reached. This control, based on the water temperature, acts accordingly to psychrometric tables and equations, so that, only the needed water steam is dragged by anode gas stream.

This is necessary because, if not enough steam is present (unless oxygen is added) the Boudouard reaction [11] could occur and give the equilibrium:

$$2CO \rightleftharpoons CO_2 + C,$$

partially converting CO into carbon, deactivating catalyst and affecting the cell performance.

1.2.3 – Testing procedure

A double step test was carried out: in the first step, only hydrogen was used to feed the stack, in order to set a benchmark for the natural gas test performance, that was the subject of the second step of the procedure.

The whole test procedure was divided into 7 subprocedures to be executed in a row. This was useful both to verify the correct fulfillment of each operation before the begin of the subsequent one, and to adapt the test sequences to the software provided with the test bench. Moreover, in case of any failure or malfunctioning of the system, the manual intervention is generally faster and less dramatic on the overall procedure.

The needed sub-procedures were identifiable as follows:

- Stack positioning,
- Leakage tests,
- Start-up and conditioning,
- Experimental measurements and characterization in hydrogen,
- Flows switch from hydrogen to natural gas,
- Experimental measurements and characterization in natural gas,
- Shut-down
- Stack removal.

The start-up procedure included the positioning and slow increase (up to 600 kgf) of a mechanical load to assure the tightening of the sealing gaskets between cells. Afterwards, anode and cathode gases are begun to flow and heat up together with the furnace at 200 °C/h.

A first gas reduction was operated as the 650 °C temperature target was reached. In steps, the conditioning mixture (5% H_2 in N_2) was converted into an intermediate mixture (up to about 33% H_2 in N_2).

The described heating up procedure is shown in **Figure 1.7**:

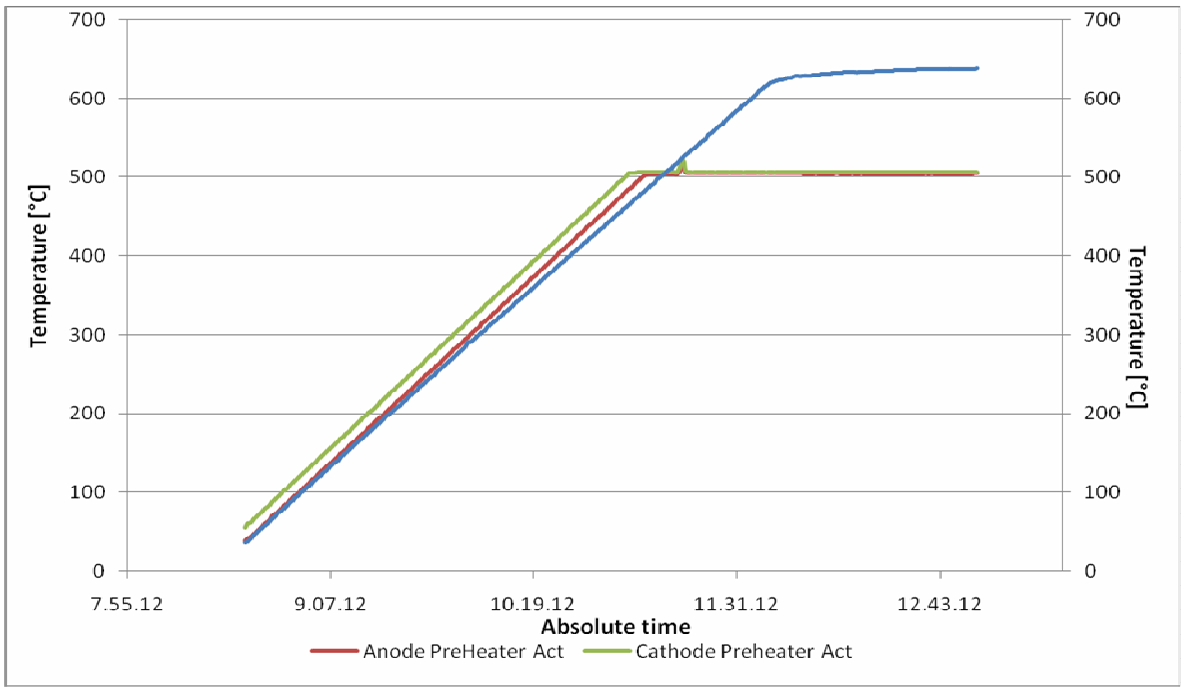

Figure 1.7: Preheating procedure at controlled temperature rate for feeding gases and furnace.

The stack was heated at 200°C/h to avoid thermal shocks to the cell that would have given damage due to the different volume mechanical expansion coefficient for temperature variation ath the electrode/electrolyte interface. This makes the startup procedure particularly long for SOFC technology. Gases were provided at 500°C, so that the cathode air flow was regulated in orde to find a compromise between temperature decreasing due to the flow and the necessity of high flow rate to have a uniform temperature distribution within the stack and to avoid limitations at high current load.

The conditioning procedure continued until temperature reached 750 °C, after that the gases were imposed at the regime flows:

H_2 flow: 2250 Nl/h (37.5 slpm), N_2 flow: 1500 Nl/h, Air flow 4000 Nl/h. From these data it is possible to calculate the stoichiometric coefficient for both anode and cathode; in particular at the maximum current value (20 A), this value, for the anode compartment (fed with H_2), is:

$$20A = 20\frac{C}{s} = 20\frac{C}{s} * 60\frac{s}{\min} = 1200\frac{C}{\min}$$

i.e.

$$1200\frac{C}{\min} = \frac{96486\frac{C}{eq} * 2\frac{eq}{mol} * \Phi_{H_2}\frac{l}{\min}}{22.414\frac{l}{mol}}$$

This calculus is for one cell only, for the whole stack it must be:

$$\Phi_{H_2} = \frac{1200 * 22.414}{2 * 96486} * 75cells \approx 10.44\frac{l}{\min}.$$

Hence, the stoichiometric coefficient is 37.5/10.44 = 3.59.

For the cathode compartment:

$$1200\frac{C}{\min} = \frac{96486\frac{C}{eq} * 4\frac{eq}{mol} * \Phi_{O_2}\frac{l}{\min}}{22.414\frac{l}{mol}},$$

as the oxygen in air is about 21%, $\Phi_{O_2} = 0.21 * \Phi_{Air}$, so:

$$\Phi_{Air} = \frac{1200 * 22.414}{4 * 96486 * 0.21} * 75cells \approx 24.88\frac{l}{\min},$$

Hence, the stoichiometric coefficient is 66.7/24.88 = 2.68.

These final flow values were set through a logarithmic gas supply reduction procedure, (i.e. with time intervals that become shorter while increasing hydrogen flow) started once the stack temperature reached an average value of 650°C.

In order to detect the correct behavior of the stack while varying the feeding mixture, the OCV was recorded and reported in **Figure1.8**. It was noticed a regular increment of the OCV in time, while increase the H_2 concentration in N_2, due to the heating process. By adopting this procedure, the mild reducing condition

allowed the anode compartment to undergo a deep reduction and hold good conductivity of the metallic component of the anode layer.

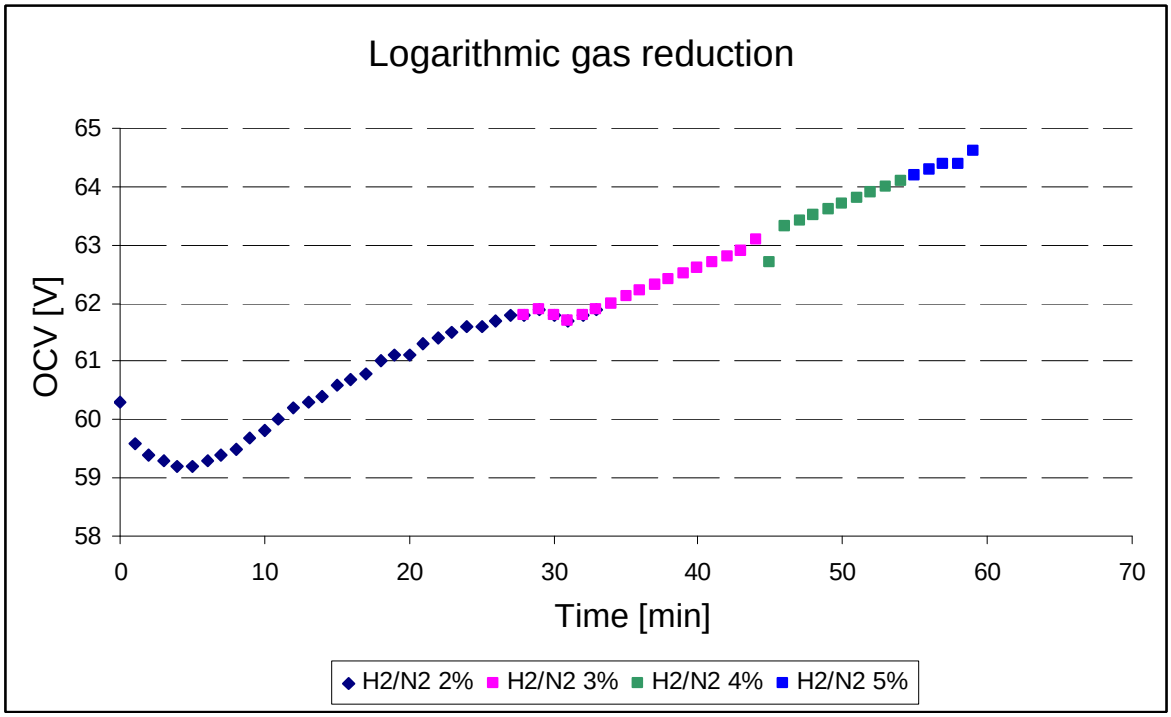

Figure 1.8: OCV variation while increasing H_2 concentration (from 2% up to 5%) in N_2 during stack conditioning, the procedure was carried out in steps with a duration variable according to a logarithmic time law.

1.2.4 - Experimental

To have a uniform distribution of temperature through the stack, a 10 A current was drained for about 30 min.

A first polarization test was performed to verify the capability of the stack of achieving the nominal 1kW power. During this test the load control mode was galvanostatic and a 16A current was drained. The overall stack voltage at each selected load is shown in **Figure1.9**.

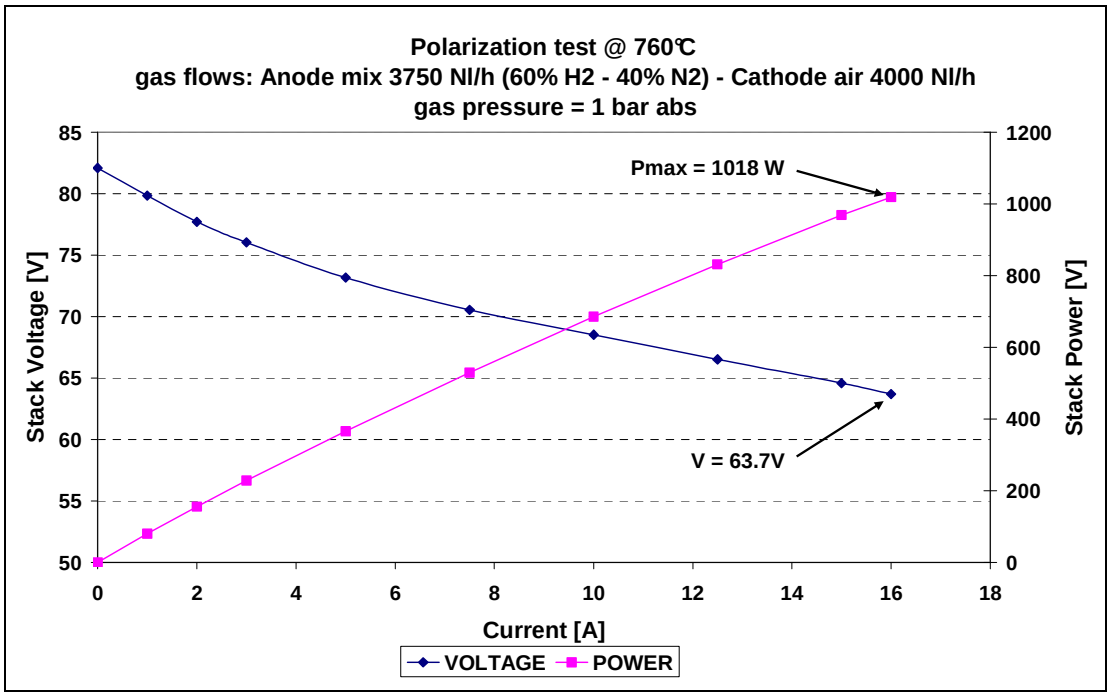

Figure 1.9: First polarization test to verify the capability of reaching the nominal power (1kW) in H_2. The expected power was generated at 16A, and the corresponding stack voltage was 63.7V.

To verify that every cell was properly working, the single cell (or ministack, according to the measurement sketched in **Figure 1.5b**) voltages were recorded and plotted in **Figure1.10**. In **Figure1.10**, it is visible a lower voltage in cell #75, on the cathode side, this is attributable to the high air flow entering the stack at a temperature lower than the cells.

After OCV stabilization, the stack underwent a second polarization test in H_2 as a benchmark to evaluate the performance in NG.

The benchmark results were extracted by performing a polarization curve from 0 to 20 A that is shown in **Figure 1.11**.

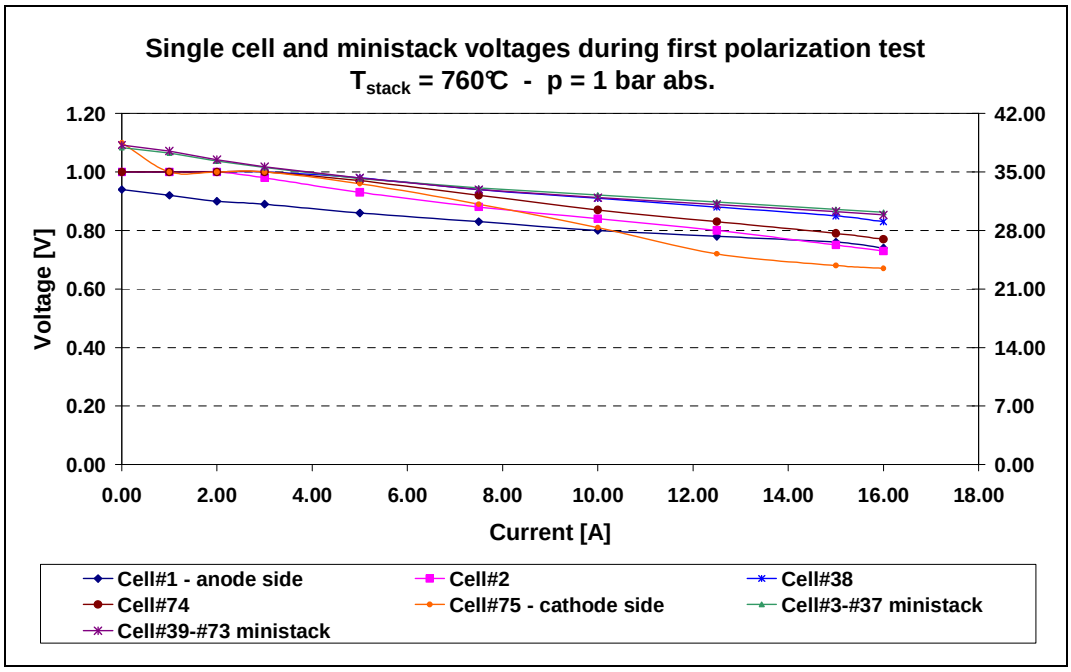

Figure 1.10: Single cell voltages recorded during first polarization test, the differences between cell voltage are not particularly significant. The lowest voltage of the cathode nearest cell may be attributable to the lower temperature in correspondance to a high a high air flow at lower temperature than the stack.

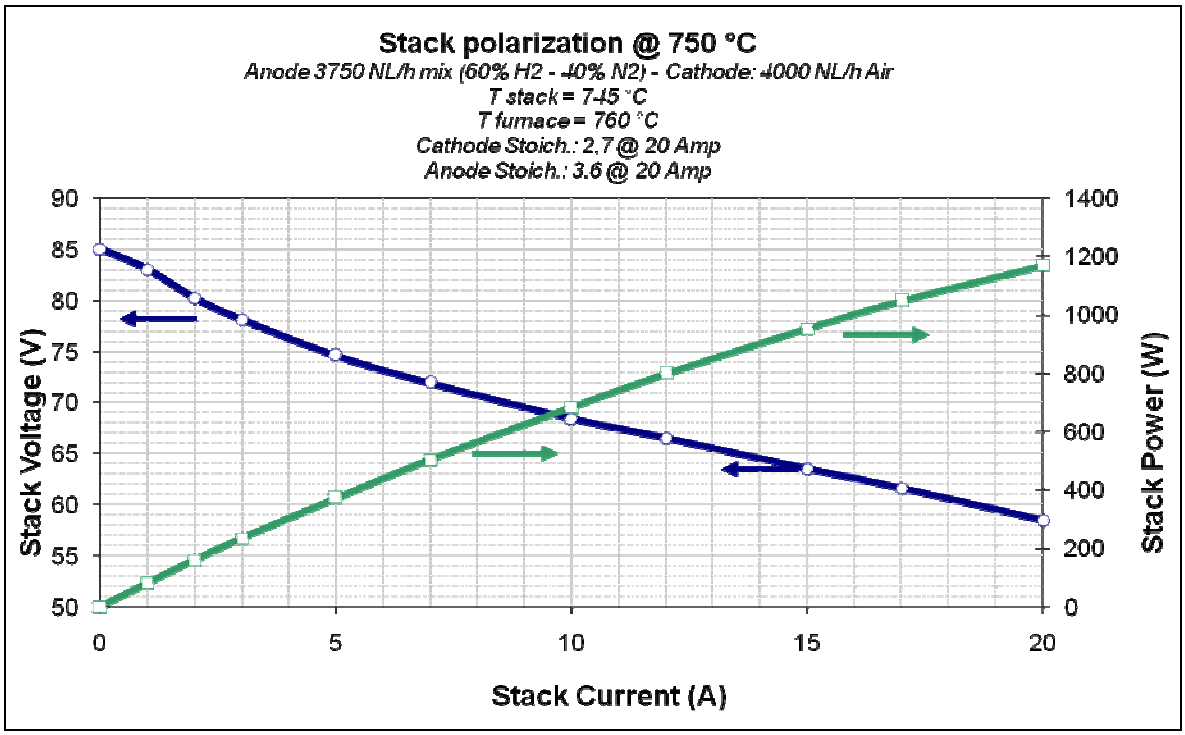

Figure 1.11: Second polarization test: OCV = 85V, P_max = 1170 W @20 A.

All polarization tests were accomplished at atmospheric pressure.

The observed OCV in hydrogen was 85.0 V. The recorded power reached a maximum value of 1170 W (measuring a voltage of 58.5 V @ 20 A), it is shown in **Figure 1.11**.

Before switching the gas mixture from H_2 to NG, the stack was loaded with a 10A constant current for 24 hours. In order to verify the correct operation in the presence of favorable feeding conditions. At the end of this procedure, a second polarization test was accomplished. The best power performance was reached, by recording a value of 1248W (corresponding to 62.43V) at 20A and a OCV = 81.58V. The IV curve and the power curve are reported (along with the ones recorded later in NG) in **Figure 1.12**.

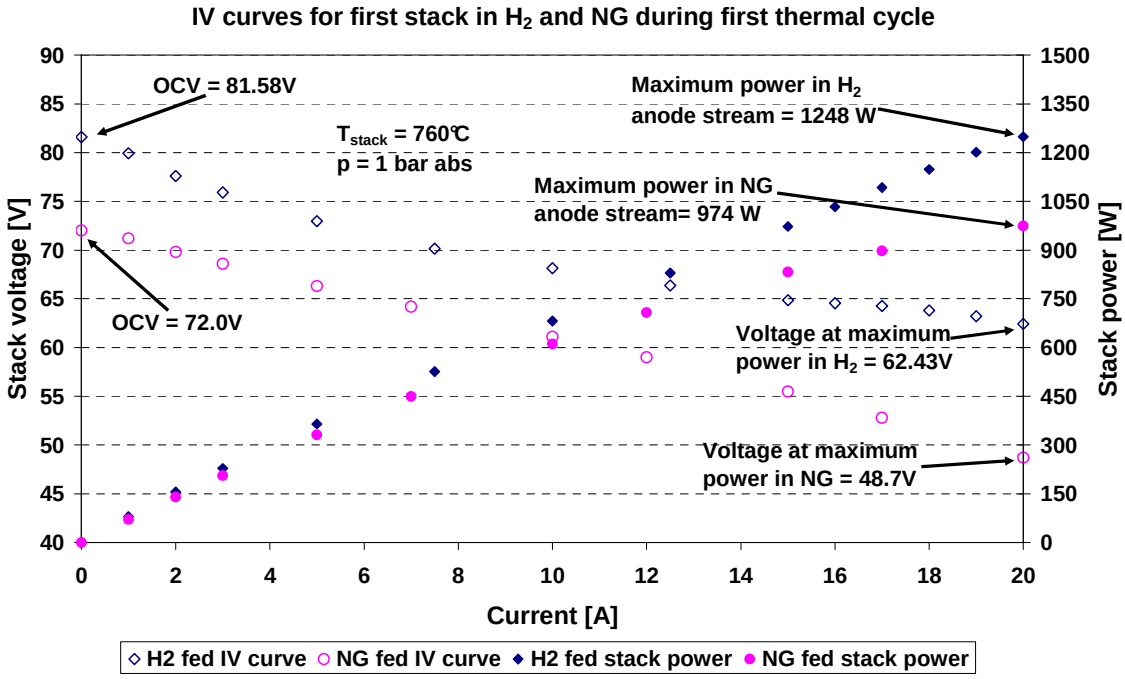

Figure 1.12: IV and power curves in hydrogen and natural gas recorded during the first thermal cycle. The stack reached very good performance with a maximum power value in H_2 of 1248W (62.43V @ 20A) and 974W in NG (48.7V @ 20A).

Once come back to 0A and after stabilizing the OCV value, the H_2 to natural gas switch was done.

Direct use of hydrocarbon fuels in SOFC stacks shows the problem of carbon deposition on a nickel based anode [12]. Carbon deposition reduces both catalyst activity and electrical conductivity; if carbon deposits create a layer, the gases will

be prevented from reacting. Moreover, carbon deposition produces mechanical strains on the anode structure and, as a consequence, the risk of cell damage.

To overcome these problems a gas pre-processing is usually applied. This can be done by an external device performing the fuel reaction with oxygen or water steam (respectively named as dry or steam reforming) and, at the outlet of the devices, a mixture of H_2, CO, CO_2, CH_4 and H_2O is collected. This device increases costs and complexity of the system.

For this stack, a two step reforming is suggested to work with natural gas. In the former step the above mentioned pre-reforming was applied; in the latter, internal steam reforming of CH_4- and H_2-rich mixture was performed.

As the reforming process is endothermic, it needs heating to be accomplished. For turnkey systems, the necessary heat is usually provided by the combustion of exhaust gases at the outlet of the stack to heat up the steam and fuel.

Due to the presence of the external pre-reforming, in this test, before starting the procedure, desulphurization and pre-reformer sections were started and set to the temperature regime conditions (respectively 330 °C and 450°C).

Moreover, the H_2 and CH_4 rich gas mixture exiting from the pre-reformer was used to feed the stack.

Three different values of steam content were used to evaluate the achievable performance with carbon deposition avoided by catalytic steam reforming, the related polarization tests are reported in **Figure 1.13**.

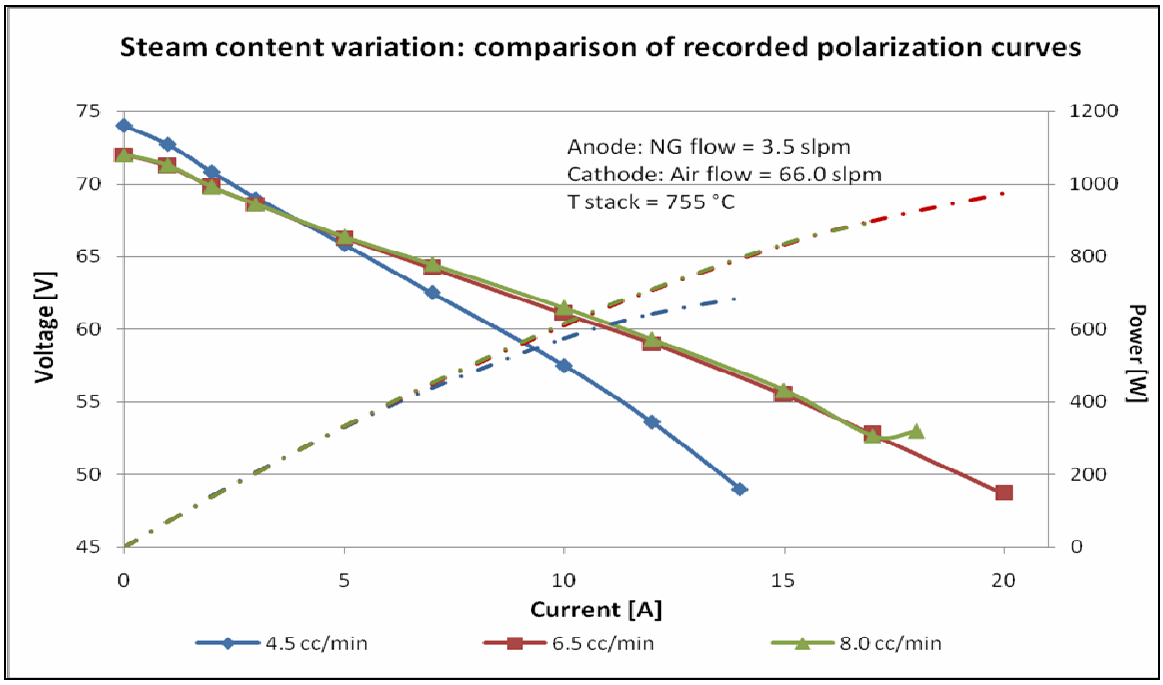

Figure 1.13: Polarization test in natural gas at variables steam content.

To investigate the effect of the variation of air stoichiometry, a steady current test was carried out. The air flow variation is shown in the following **Table 1.2**:

Air flow[slpm]	Voltage [V]	Stack Temp. [°C]
66.7	52.4	756
83.3	51.6	756
100.0	49.7	756
116.7	46.5	755
133.3	42.5	753
100.0	43.6	751
66.7	47.2	751

Table 1.2: Recorded stack voltages and temperatures at different air flows.

A slight temperature variation was observed, but the stack voltage appeared to have significant sensitivity to the excess of air. This flow caused a rapid cooling of cathode feeding gas. As a compromise, it was chosen an air flow of 66.7 slpm corresponding to a stoichiometry of 2.7 at 20 A.

1.2.5 – Natural gas fed SOFC time test

A 161 hour (about one week) time test was carried out by draining a 14 A constant current. During this test, the stack continuously produced about 730W (i.e. 52.3 V). This power was recorded without any significant fluctuation and in stable condition of feeding gases and mechanical load. This result was comparable with that achieved in pure hydrogen. The difference in current value of 14 A instead of 16 A with respect to the test in H_2 was selected to diminish the risk in natural gas of reaching the cutoff voltage.

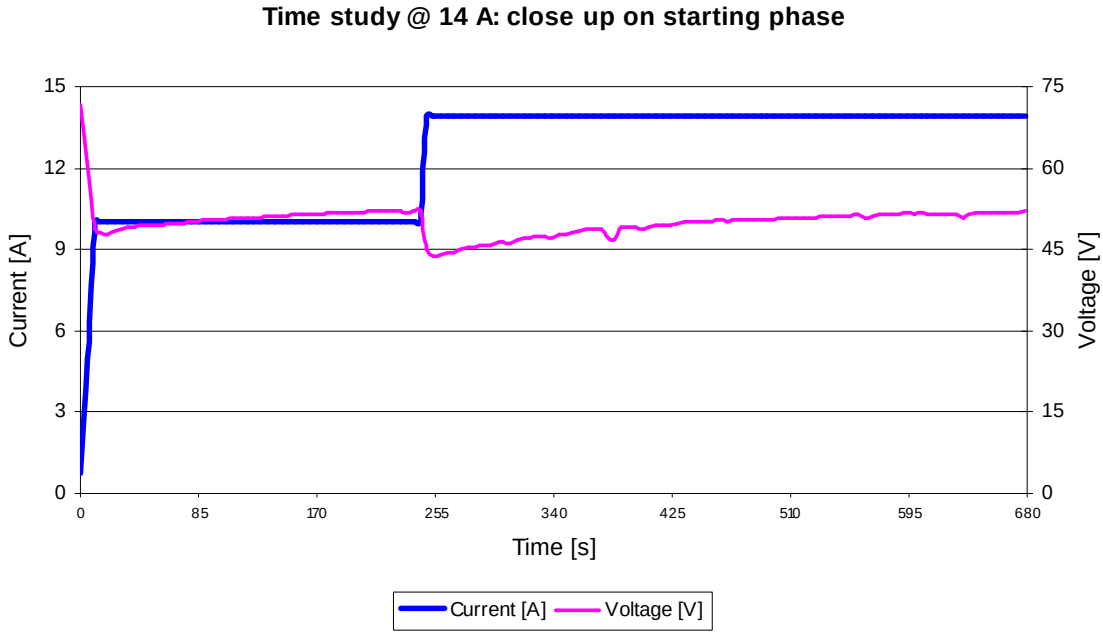

Figure 1.14: Transient behavior at the beginning of the time study at 14 A constant current, the maximum current value was reached in two steps.

As shown in **Figure 1.14** the time study was performed in two steps: the former was 4 minute long at 10 A to give a uniform distribution of temperature in the stack (from anode to cathode), and, as this steady condition was reached, the latter step was started. The first recorded voltage value was 43.7 V. An increase of voltage in the first few minutes is reported in the following **Table 1.3**:

Time [min]	Voltage [V]
0	43.7
1	46.8
2	48.8
3	50.1
4	50.6
5	51.2
6	51.5
7	51.9

Table 1.3: Recorded voltages during transient phenomena at 14 A.

The long run of the time study yielded the steady current voltage trend, this is shown in **Figure 1.15**, the average recorded value is 52.09 V and it is possible to observe a very slightly increasing value of the stack voltage of about 20 µV/min.

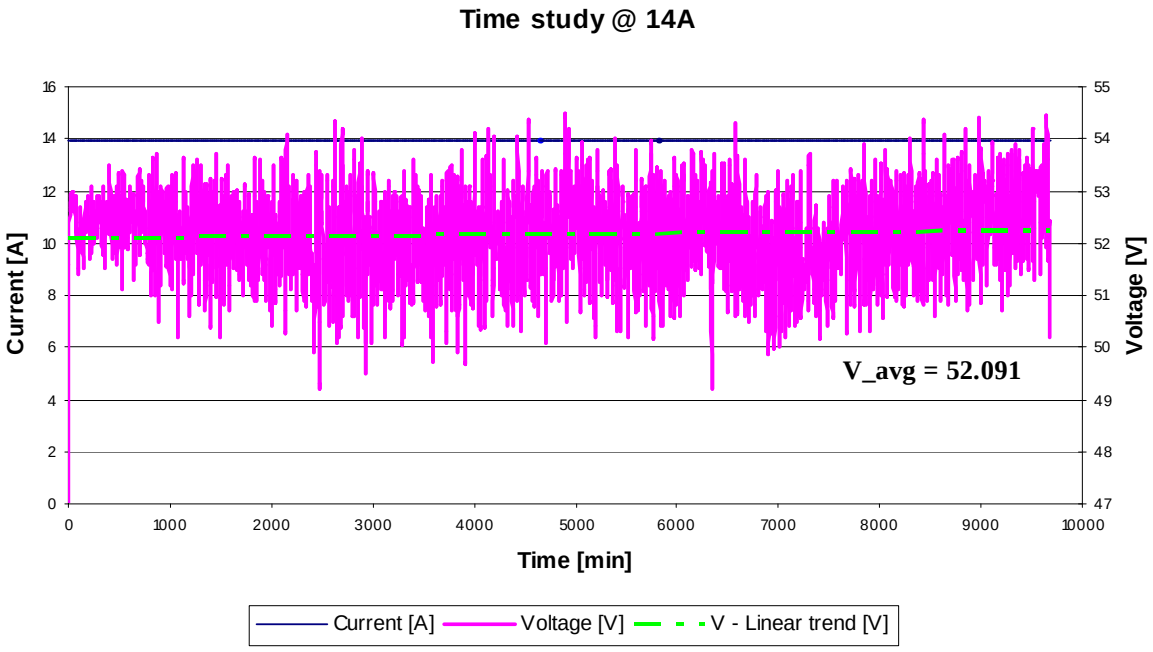

Figure 1.15: Endurance test at 14 A to analyse stack voltage stability and linear trend.

At the end of this test, a slow current reduction was executed down to 0 A to measure the new OCV value, and a value of 74.0 V was recorded in natural gas.

After that, a second endurance test was carried out, the result of the starting operations is reported in **Figure 1.16** (and significant points in **Table 1.4** as well) and shows increased values of voltage with respect to the same current values of

the previous test. To have a comparable start conditions, a long conditioning in hydrogen was done.

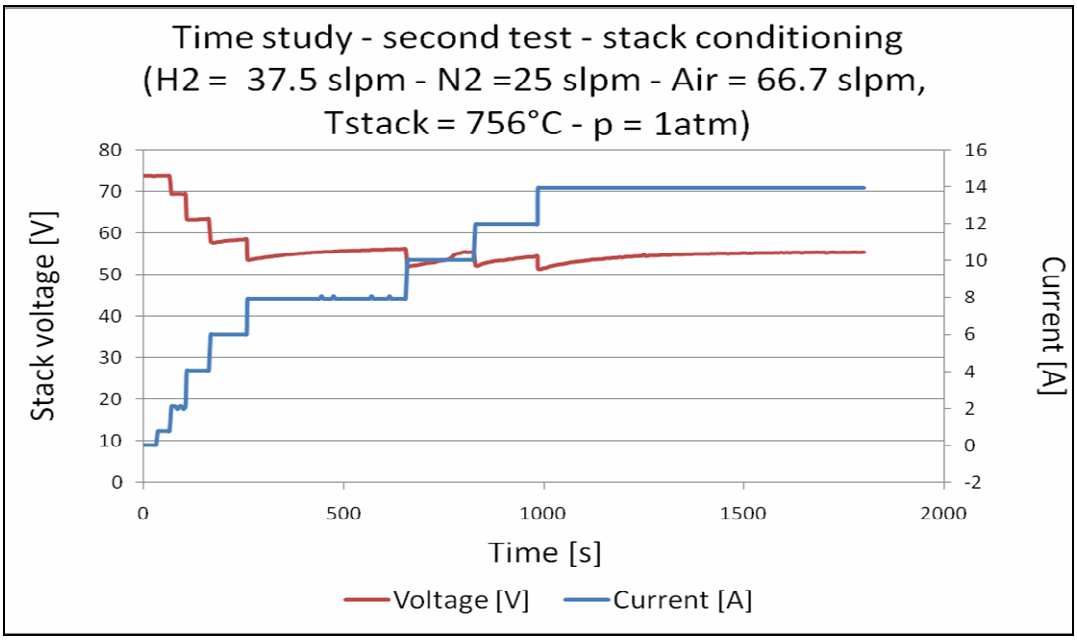

Figure 1.16: Second time study, maximum current (14 A) reached in several steps.

Time [s]	Current [A]	Voltage [V]
0	0	74
40	0.75	73.8
84	1.95	69.4
120	4.05	63.3
180	6	57.9
232	6	58.3
289	7.95	53.9
349	7.95	54.7
529	7.95	55.8
709	10.05	52.8
799	10.55	55.4
829	12	52
889	12	53.4
979	12	54.4
1005	13.95	51.6
1035	13.95	52.4
10.95	13.95	53.2
1185	13.95	54.1
1425	13.95	55

Table 1.4: Significant point at increasing current values during tests after a thermal cycle.

After about 29 hours the feeding gas was switched in natural gas and water steam, the transient phenomenon is reported in **Figure 1.17**. It showed a decrease in the average voltage value with respect to the one recorded in hydrogen. Moreover, during the transient it was possible to observe the short term effect of water steam as fluctuations of the voltage value and the related variation from 2.4 cc/min to 4 cc/min and to 6.6 cc/min.

Usually, by calculating the ratio between number of moles of steam and number of moles of carbon, it is defined a steam/carbon (S/C) ratio; the considered water content correspond respectively to: S/C=2, S/C= 3.33 and S/C=5.5.

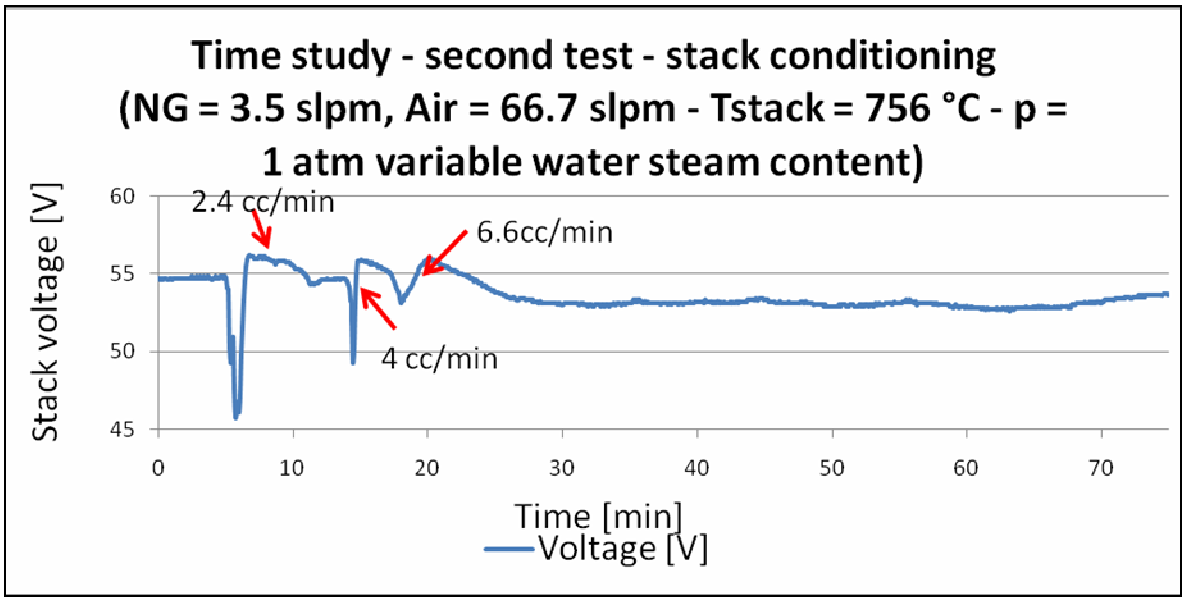

Figure 1.17: Effect of the steam content variation at the beginning of the second time study. The water addition is necessary to supply the stack with enough oxygen to avoid carbon deposition; on the other hand, this produces lowering of the anodic potential. For this reason, it is necessary to find a good compromise between these two contrasting phenomena. The corresponding steam-to-carbon ratios (S/C) were taken between 2 and 5.5.

The voltage fluctuations are attributable to the O_2 presence in anode stream (coming from water steam) whose effect is reducing power of the anodic stream; on the other hand, the water steam makes possible the steam reforming reaction.

Different water contents in gas flow were attempted to find a good compromise between voltage reduction (with respect to pure H_2 feeding) and

voltage stability (affected by the endothermic equilibrium of reforming reaction, especially at low current load).

In **Figure 1.18** it is possible to observe the effect of the short second conditioning in little amount of hydrogen between two long run in natural gas.

The stack has shown a 2-volt voltage recovery with respect to the previous endurance test, the average recorded value is 53.95 V instead of 52.09 at 14 A, moreover the voltage trend appears to show an increasing behavior.

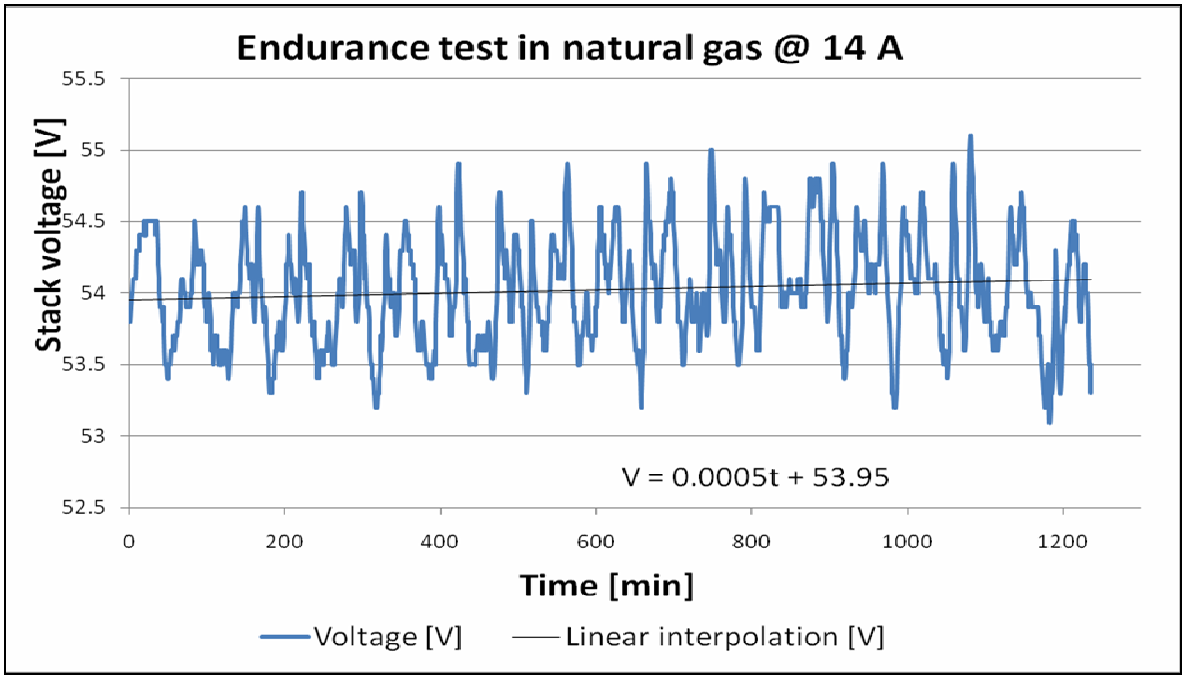

Figure 1.18: Endurance test in natural gas at 14 A and linear trend approximation. The plotting vertical scale highlights that fluctuations are not more than 1V around the average voltage during the whole 20 hour test.

After the 20 hour test at 14A load, the stack underwent a controlled shut down (carried out at 5°C/min, according to the manufacturer spcifications) to study its behaviour if a thermal cycle occurs.

After complete cooling, the start-up procedure was started again; the subsequent polarization test was quite satisfactory, reaching power performance similar to the the one achieved in the previous tests both in hydrogen and in natural gas, as shown in **Figure 1.19**, with a maximum value of about 1108W at 18A in hydrogen and 867W at 15A in natural gas. These values are very close to

the ones recorded during the first thermal cycle (1170W, at the same current loads), highligthing no significant decay caused by this shut-down/start-up operation. The relative performance decay is (1170-1108)/1170=0.053=5.3%. This decay does not seem a dramatic value, provided that any operation in H_2 was not carried out (unlike it was done when best performance was recorded in the previous cycle).

The results were normalized (**Figure 1.20**) with respect to number of cells in the stack and cell area to be easily comparable with the other solid oxide fuel cell based devices.

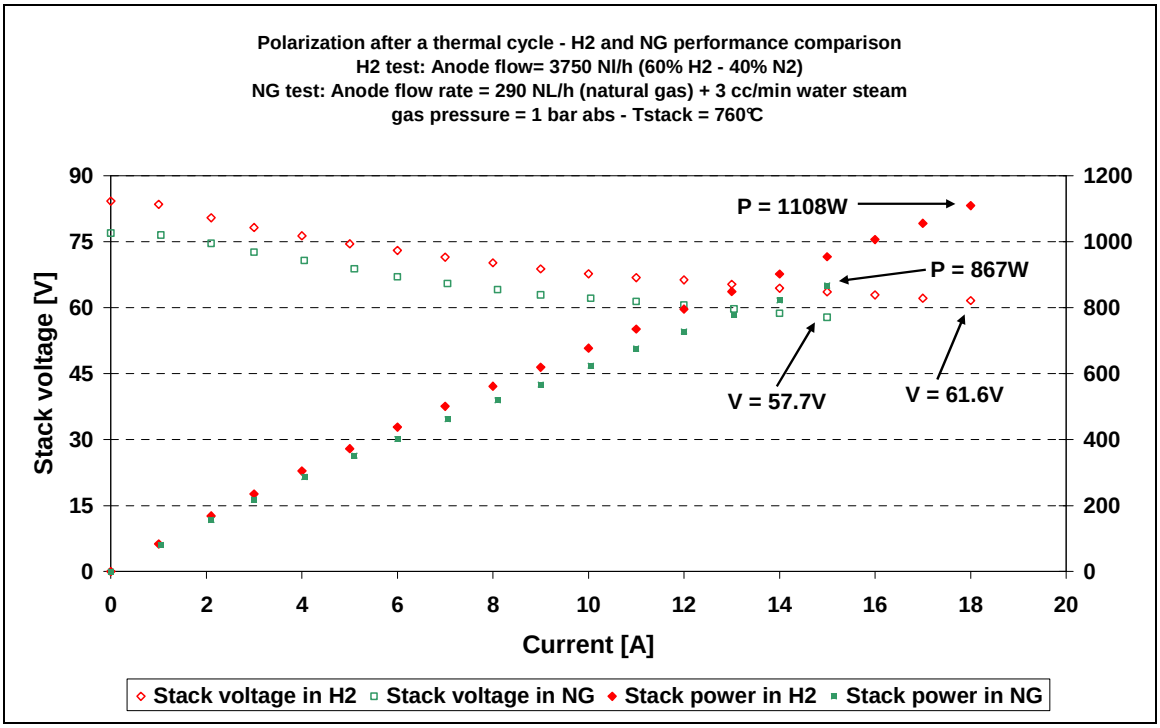

Figure 1.19: Performance comparison between H_2 and NG fed polarization tests. The maximum power difference can be attributable to the different thermodynamic potential of NG and H_2, and the ohmic region of the IV curve showed similar slope, so that no degradation of electrolyte can be detected after short endurance test in H_2.

As visible in **Figure 1.21** (in which the overall stack and gases temperature behaviours are reported) the stack was operated at 760°C feeding gas streams at 650°C.

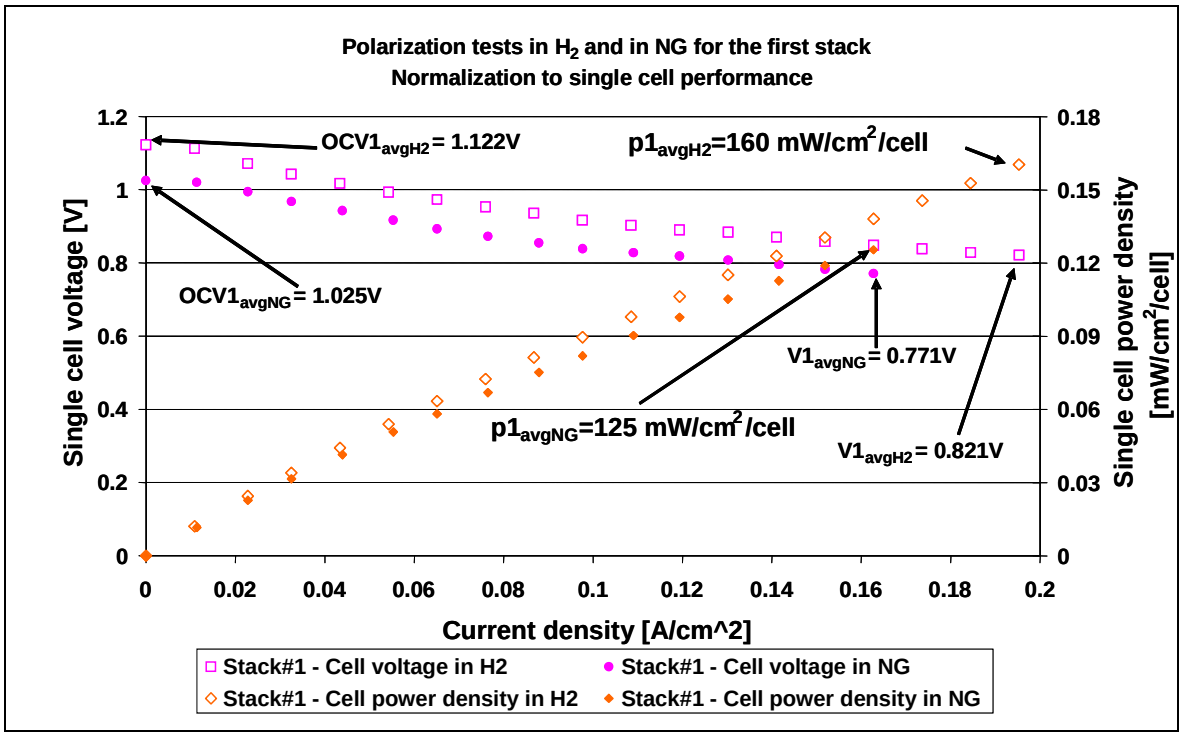

Figure 1.20: Normalized results of polarization tests both in H_2 and NG for the first stack operating in the second thermal cycle.

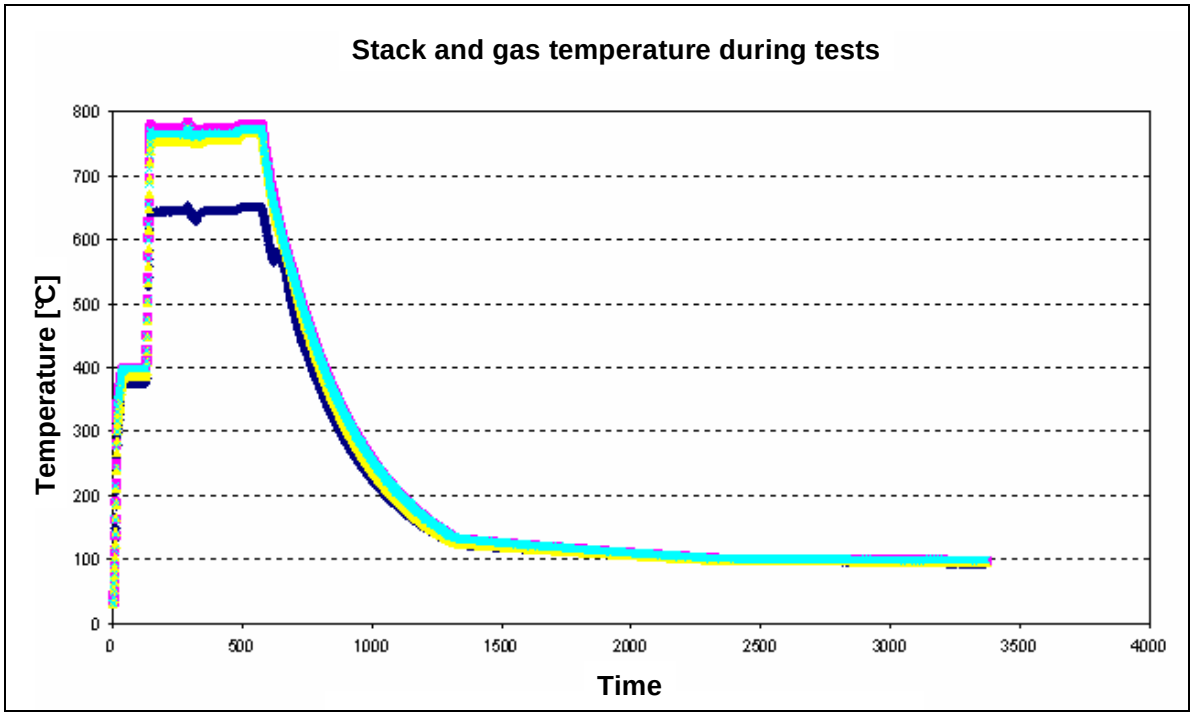

Figure 1.21: Overall temperature log for stack and gases during the whole second thermal cycle; the rightmost part of the figure represents the stack cooling/shutdown, the negative temperature slope was limited by the furnace insulation.

1.2.6 - Conclusions

A planar SOFC stack was tested by polarization and endurance tests. It was fed with either hydrogen or natural gas and thermal cycles were performed. A good voltage stability under steady state conditions was observed. Thermal cycles slightly affected the power performance. A short conditioning in hydrogen appeared as a process allowing to recover good efficiency. By applying this procedure, even a higher voltage value (at same current load) was recorded after the latter thermal cycle. Different water steam contents in natural gas were investigated; the steam showed a valuable contribution to avoid carbon deposition on the anode catalyst without affecting the generated power

1.3 - Catalytic partial oxidation based 1kW planar SOFC stack

1.3.1 - Introduction

With the purpose of evaluating two different approaches to the market related issues, a second commercial stack was tested. This new stack was chosen thanks to two differences with respect to the previous. In this case, the selected stack shows two advantages, the former is a self compression system, so there is no need for external compression plunger in the turnkey system, the latter is the way to adapt the stack power to the customers' demands.

In particular, single cells are packed in clusters with 6 cells each, so, once assembled every cluster, the tightness of the gaskets must be assured only between the plates at the extremes of each cluster.

Moreover, from the scale-up strategy point of view, to match demands of different residential units, the choice of stackable cell clusters as pre-fabricated devices, allow for adaptation to different nominal power values. Furthermore, in case of damage of the stack, that typically involves contiguous cells, the replacement of one whole cluster in a single operation leads to reduction of plants shutdown time.

The latter difference is the presence of a self-compression strategy for each cluster. In fact, every group of six cells is packed with sealing and removable

springs to hold the whole cluster. For stack configurations, two holes through every cell are exploited by inserting threaded rods with calibrated springs to give a proper tightness and assure avoidance of gas leakage.

1.3.2 – Stack description and operating procedure

The stack consisted of 72 anode supporting planar cells in series and enclosed in a metal shell (visible in **Figure 1.22**) provided with insulating material to avoid short circuits and offer mechanical protection to the cells. Each cell has an area of 50cm^2. N-type thermocouples were mounted to monitor the temperature distribution during operations.

Figure 1.22: Second tested stack. Composed of 75 cells, it is enclosed in a protective shell and has a self compressione system made with threaded rods and calibrated springs.

This stack operated at about 760°C at a pressure of 1 bar abs. After a start-up procedure comparable to the one applied to the first stack, and whose temperature trends are reported in **Figure 1.23**, both in terms of time duration and H_2/N_2 feeding mixture, two polarization tests were carried out.

The only significant variation in the start-up procedure was the gas temperature at the inlets, it was set at 750°C instead of 650°C.

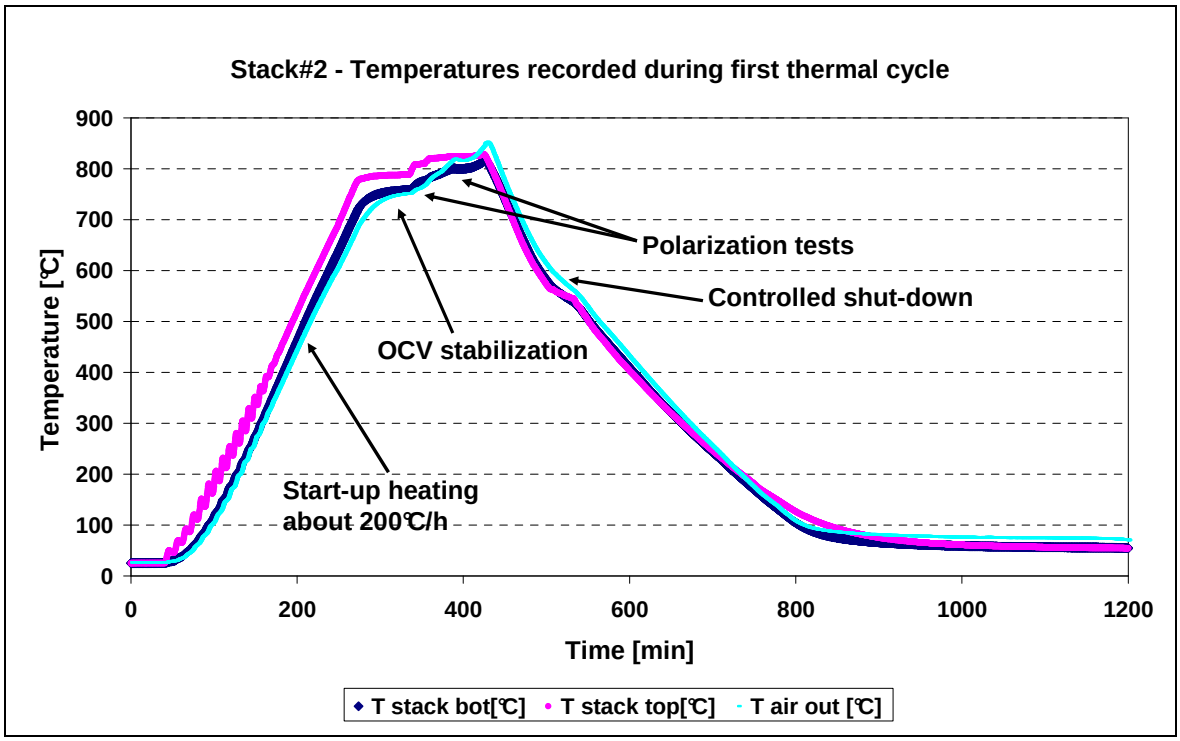

Figure 1.23: Temperature behaviours into the stack shell during the whole test. It is possible to tell the heating up for stack conditioning, the two time intervals used to carry out two polarization tests and the shutdown operation.

Moreover, this stack operated a dry reforming process, by adding oxygen (by air) in the anode stream. This is a catalytic partial oxidation (CPOx) reaction i.e. the oxygen content in the anode stream is lower than the stoichiometric amount for full oxidation. This process allows for a better compactness of the whole gas processing system and for reduced hardware complexity. It is a catalytic reforming process so that CH_4 and H_2 mixture (from natural gas) reacts with oxygen according to the reactions:

$$CH_4 + 1/2\ O_2 \rightleftharpoons CO + 2H_2$$

and

$$CH_4 + 2\ O_2 \rightleftharpoons CO_2 + 2\ H_2O,$$

depending on the thermodynamic conditions, CO_2 can continue to react with CH_4, according to:

$$CH_4 + CO_2 \rightleftharpoons 2\ CO + 2H_2.$$

Since these reactions reflect a dynamic equilibrium, the produced CO is further converted in CO_2 by preferential oxidation (PrOx) using the O_2 content of the anodic air flow:

$$2\,CO + O_2 \rightleftharpoons 2\,CO_2.$$

This process is advantageous with respect to steam reforming because there is no need for humidification management (so an intrinsic cost reduction is achieved reducing auxiliary devices) and has higher reaction rates than steam reforming.

The addition of little oxygen flow at the anode avoids the occurrence of two detrimental reactions [13]:
the pyrolysis of the methane, according to:

$$CH_4 \rightleftharpoons C + 2\,H_2$$

that gives carbon fibres deposits on the anode catalyst, and the already mentioned Boudouard reaction:

$$2CO \rightleftharpoons CO_2 + C.$$

Moreover, high temperature provides thermodynamic conditions to avoid a secondary effect of the presence of the produced CO_2:

$$CH_4 + CO_2 \rightleftharpoons 2\,C + 2\,H_2O$$

About the environmental protection, as per the above mentioned reactions, CO_2 can be re-used as a reactant for hydrogen production and greenhouse gas reduction is obtained. On the other hand, dry reforming shows lower yield of H_2 per carbon content in fuel. In more details. the conversion efficiency in the mixture depends on the O_2-to-CH_4 ratio and on the processing temperature. It must be noticed that, even if the reactor temperature is initially regulated, the O_2-to-CH_4 ratio influences the temperature into the CPOx reactor by affecting the heat production of the process.

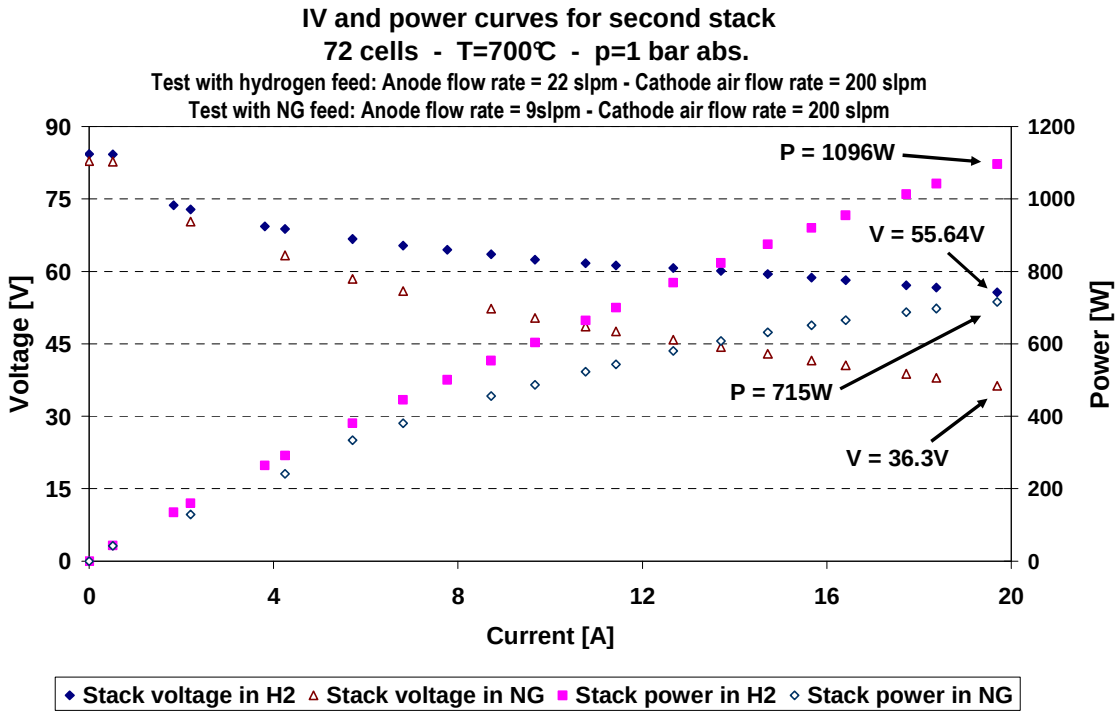

Figure 1.24: IV curves of second tested stack, recorded in hydrogen and natural gas. The stack showed a maximum power in hydrogen higher than 1kW, but it had a significant power loss in natural gas. This loss may be attributable to high ohmic resistance. Anyway both test appeared valuable once considered the small cell area (about 50cm²) and the necessary oxygen presence for CPOx to avoid carbon deposition in the long run.

As shown in **Figure 1.24**, the stack achieved a maximum power value of 1096W in hydrogen and 715W in natural gas. The difference is attributable to a lower reaction rate of natural gas, even in the presence of dry reforming. In comparison with the first stack, it must be considered the difference of about 50°C in operation. Thus, a part of the performance difference was due to the lower catalyst performance at that temperature.

The recorded OCVs were 84.32 V and 82.89 V, respectively for H_2 and NG (that correspond to 1.17 V and 1.15 V per cell, as visible in **Figure 1.25**, where normalized values with respect to number of cells in the stack and cell area are reported).

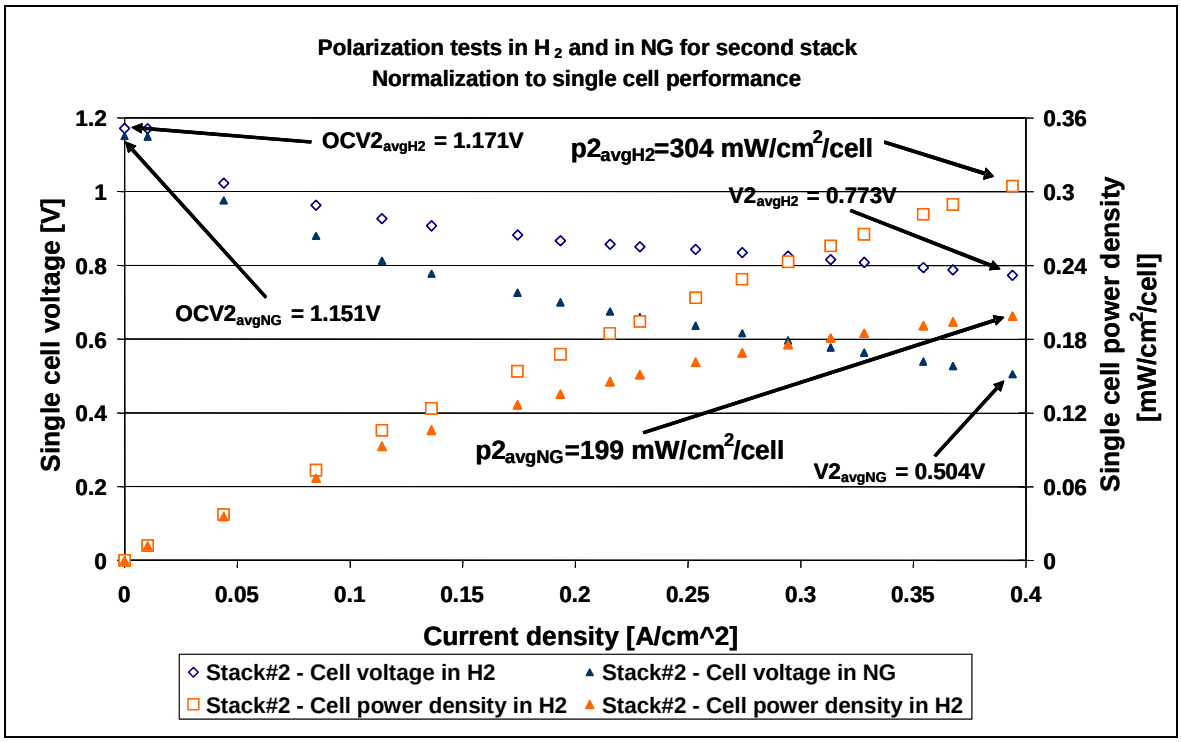

Figure 1.25: Normalized results of polarization tests both in H_2 and NG for the second stack.

A second cause of the performance loss can come from the oxygen presence in the anode stream. This lowered the oxidation potential of hydrogen (and residual methane).

1.4 – Results comparison

In order to compare the results of performance tests, a re-scaling must be executed; in fact the two stacks differ in terms of number of cells (to compare voltages) and single cell area (to compare current load). These properties are summarized in **Table 1.5**:

	STACK#1	STACK#2
Number of cells	75	72
Surface area [cm²]	92.16	50
Working temperature [°C]	760	760
Anode gas flow rate (H_2) [slpm]	37.5	22
N_2 flow rate (in H_2 mixture) [slpm]	25	0
Anode gas flow rate (NG) [slpm]	3.8	4.8
Cathode gas flow rate (Air) [slpm]	66.7	200

Table 1.5: Summary of the main physical and operative parameters for the two stacks.

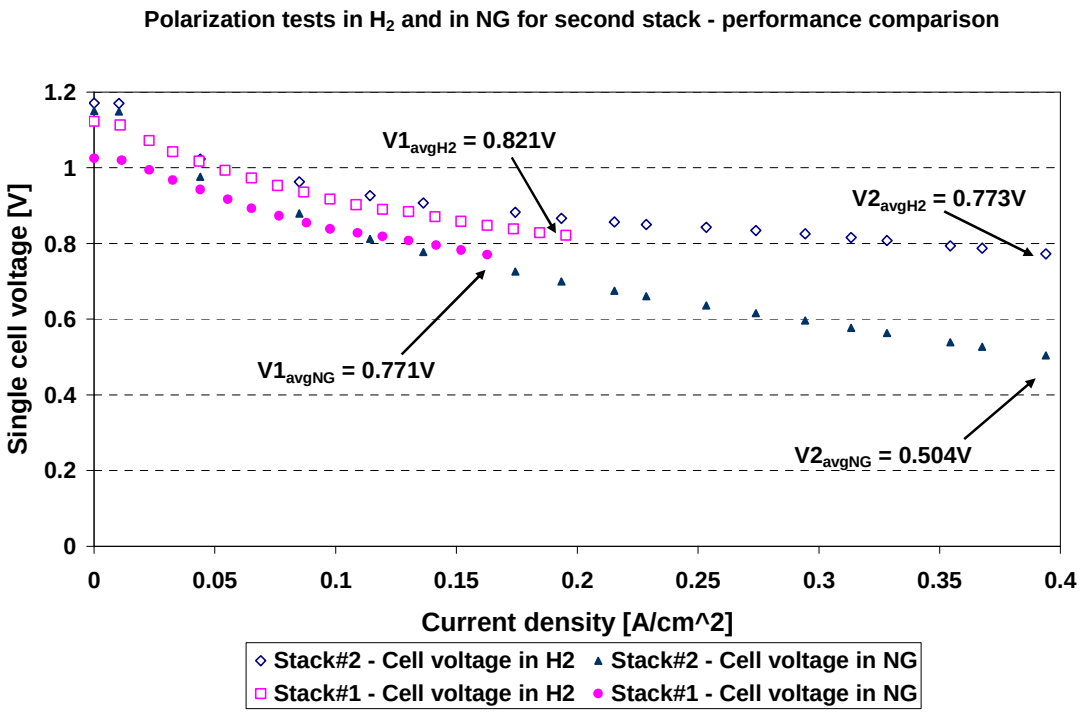

Figure 1.26: IV curve comparison for the two stacks with hydrogen and natural gas feeding. To have a clear comparison, the curves were normalised with respect to the nuber of cells (by representing the average cell voltage on the vertical axis) and to the cell area (by representing the current density on the horizontal axis).

For this reason, to have a fast comparison between the performance of the two stacks, in **Figure1.26** and **Figure1.27** single cell average voltage and power density per cell were, respectively, reported in vertical axis; likewise, on the horizontal axis current density is considered.

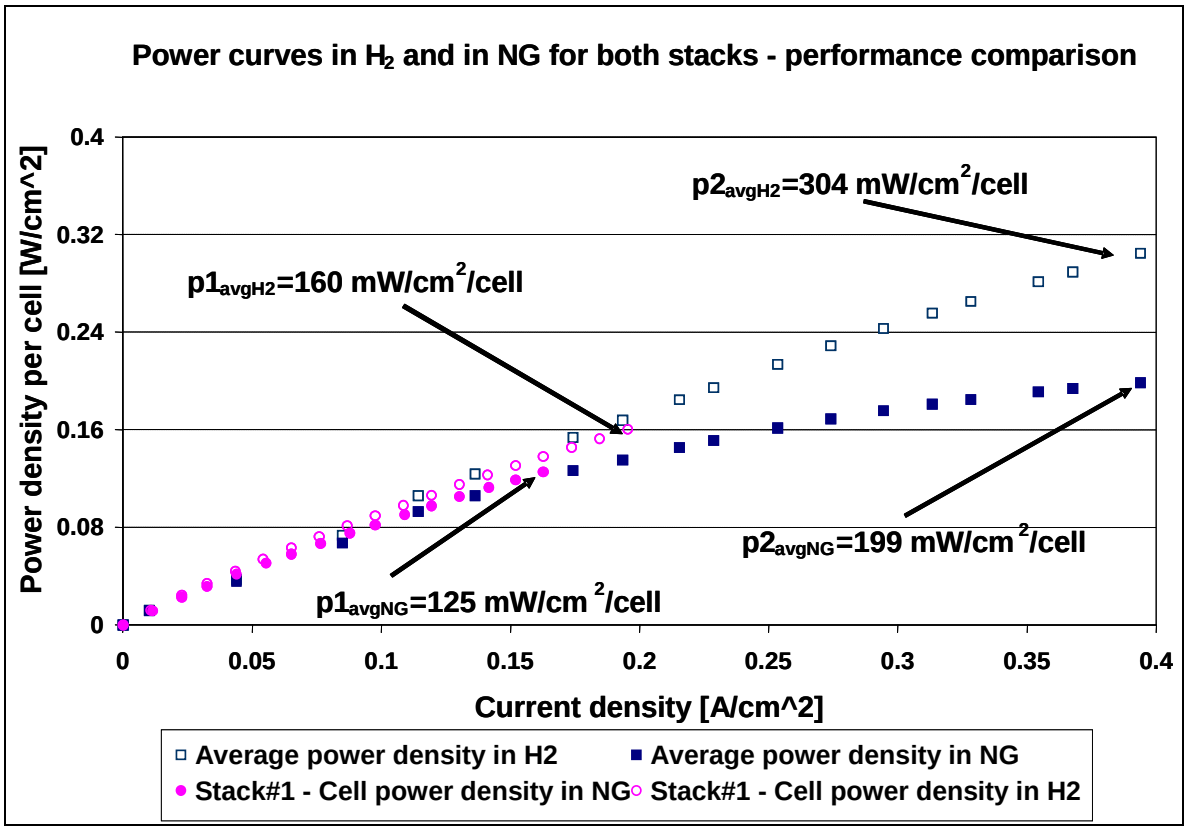

Figure 1.27: Power curves comparison of the two stacks. The visual comparison clearly shows a superior power density of the second stack at maximum current density, but there are not differences at equivalent current density.

In **Figure1.27**, it is visible that both stacks reached similar power density at equivalent loads, but Stack#1, due to its size can be still used in order to achieve power values higher than its design target. Likewise, Stack#2 achieved a higher specific load both in hydrogen and in natural gas. Anyway, it must be considered that both stacks were not brought below minimum cell voltages for safe operation. This allows to envisage that Stack2 reaches higher performance according to nominal characteristics declared by the manufacturers, but unfortunately only 1 thermal and redox cycle was assured. On the contrary, Stack1 has (besides the possibility to deliver higher power) the capability of coping with some thermal cycles, and operation in hydrogen can recover possible performance decay after natural gas operation.

1.5 - References

[1] R. J. Gorte, S. Park, J. M. Vohs, C. Wang, Advanced Materials, 12, No. 19, October 2, 2000.

[2] S. Tao and J. T. S. Irvine, Nature Materials, 2, 320-323 (2003).

[3] T. Hibino, A. Hashimoto, M. Yano, M. Suzuki, M. Sano, Electrochimica Acta, 48, 2531-2537 (2003).

[4] M. Lo Faro, D. La Rosa, G. Monforte, V. Antonucci, A. S. Arico and P. Antonucci, Journal of Applied Electrochemistry, in press.

[5] J. V. Herle, T. Horita, T. Kawada, N. Sakai, H. Yokokawa, M. Dokiya, Ceramic International, 24, 229-241 (1998).

[6] A. Sin, E. Kopnin, Y. Dubitsky, A. Zaopo, A. S. Aricò, L. R. Gullo, D. La Rosa, V. Antonucci, Journal of power Sources, 145, 68-73 (2005).

[7] Y. Ji, J. A. Kilner, M. F. Carolan, Journal of the European Ceramic Society, 24, 3613-3616 (2004).

[8] R. Burch, M. J. Hayes, Journal of Molecular Catalysis A: Chemical, 100, 13-33 (1995).

[9] O. A. Marina, M. Mogensen, Appl. Catalysis A: General, 189, 117-126 (1999).

[10] Brunaccini, G., Lo Faro, M., La Rosa, D., Antonucci, V., Aricò, A.S. (2008) International Journal of Hydrogen Energy, 33 (12), pp. 3150-3152.

[11] Moon D.J. – Catal Surv Asia (2008) 12:188-202

[12] Effects of dilution on methane entering an SOFC anode Journal of Power Sources Volume: 106, Issue: 1-2, April 1, 2002, pp. 323-327 Kendall, K.; Finnerty, C.M.; Saunders, G.; Chung, J.T.

[13] Equilibria in fuel cells - Sasaki, Teraoka - Journal of the electrochemical Society, 150 (7) A885-A888 (2003).

Chapter 2

HT-PEM stack characterization under significant working conditions for automotive applications

2.1 - Background

The study of new types of electrolyte membranes and catalysts may offer a solution for the automotive application of polymer electrolyte membrane fuel cells (PEMFC). The main problems are related to the operating temperature range (usually considered both too low and narrow) and the high membrane humidification.

Although currently standard membrane materials, i.e. Nafion, have good proton conduction and chemical stability over time when highly humidified, they show some critical limitations when relative humidity decreases. This evidence makes the overall system more complex and expensive due to the necessity of an appropriate water and thermal management. Moreover, a variation of these working conditions (temperature and humidification) causes mechanical stress on the membrane due to the volume shrinking when them are significantly (even locally) dried with consequent irreversible damage.

Based on these considerations and in the framework of an EC project ("Autobrane"), this reported activity aims at studying a new membrane-electrode assembly (MEA) technology and its practical application in relevant automotive operating conditions, through testing of large area short stacks.

In particular, in this year of activity, performance tests were carried out in a wide range of working conditions, different electrocatalysts were evaluated to find the best performance in automotive relevant environment.

2.2 - Description of work

The aim of this work was to investigate the behaviour related to high temperature operations (130°C) of innovative large area (360 cm^2) membrane-

electrode assembly (MEAs) in a practical stack hardware (bipolar plates and end-plates) provided by Nuvera. Steady-state operation, endurance and accelerated tests were carried out in a small single cell (5 cm^2) on two different MEA preparations at 80 ° and 130 °C in order to make a screening of the hardware components and MEA materials.

The MEAs were prepared at the CNR-ITAE Institute in the framework of the Autobrane project. These MEAs consist of highly dispersed Pt metal particles on two different carbon supports characterized by a high surface graphiticity index to sustain high temperature operations i.e. Ketjen Black (KB) and Carbon Vulcan (CV). To achieve proper degree of dispersion for Pt, it was necessary to decrease the metal concentration on Vulcan from 50 to 30%.

2.3 - Physico-chemical investigation

Physico-chemical characterizations were performed to better evaluate the effect of the degradation/dissolution of the catalysts during operation as well as swelling of the membrane.

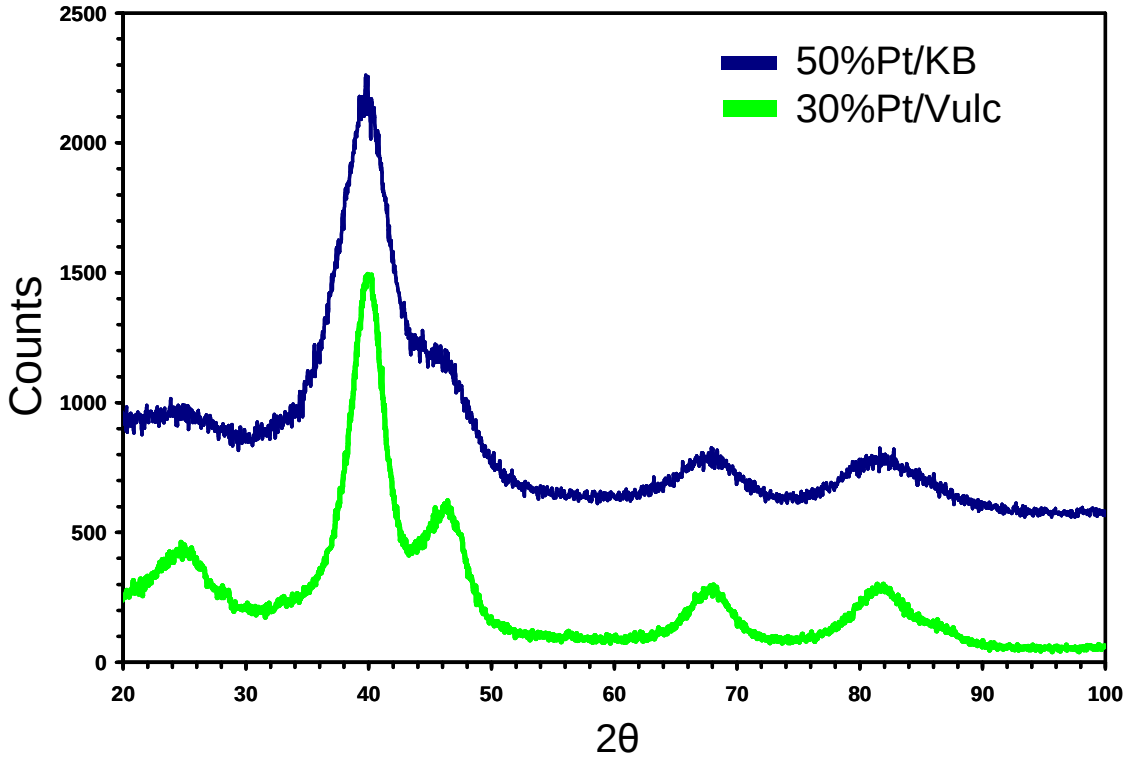

Figure 2.1: typical peak patterns of Pt FCC structure

These preliminary analyses allowed to have a first screening of the MEAs to individuate the critical aspects that have to be addressed at high temperature working conditions.

In particular, XRD patterns for both electrocatalysts were recorded and reported in **Figure 2.1**. The diffraction peaks confirmed the presence of Pt metal on the carbon support.

Moreover, to investigate on the Pt distribution on carbon, TEM pictures were taken. Those pictures (**Figure 2.2**) showed appropriate dispersion on fresh samples (in shape of powder) and highlighted the absence of any significant agglomeration of Pt particles.

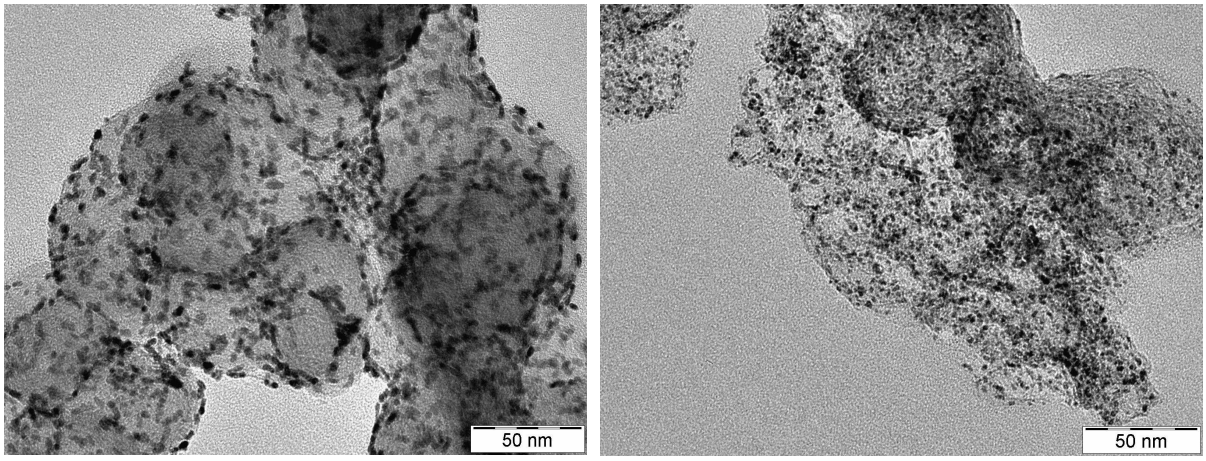

Figure 2.2: TEM pictures of electrocatalyst distribution before (fresh powder sample) on the carbon support for 30%Pt/CV (a) and 50%Pt/KB (b) preparations

2.4 - Electrochemical characterization of single cells

Electrochemical characterizations were carried out for 50%Pt/KB and 30%Pt/CV MEAs in a single cell commercial hardware of 16 cm^2 provided by Nuvera. In **Figure 2.3** polarization curves at 80°C before and after stability test at 0.7 V are reported, an opposite behaviour of the recorded voltage is visible for the two cells. High pressure (3 bar abs) in the anode and cathode compartments was used for all experiments.

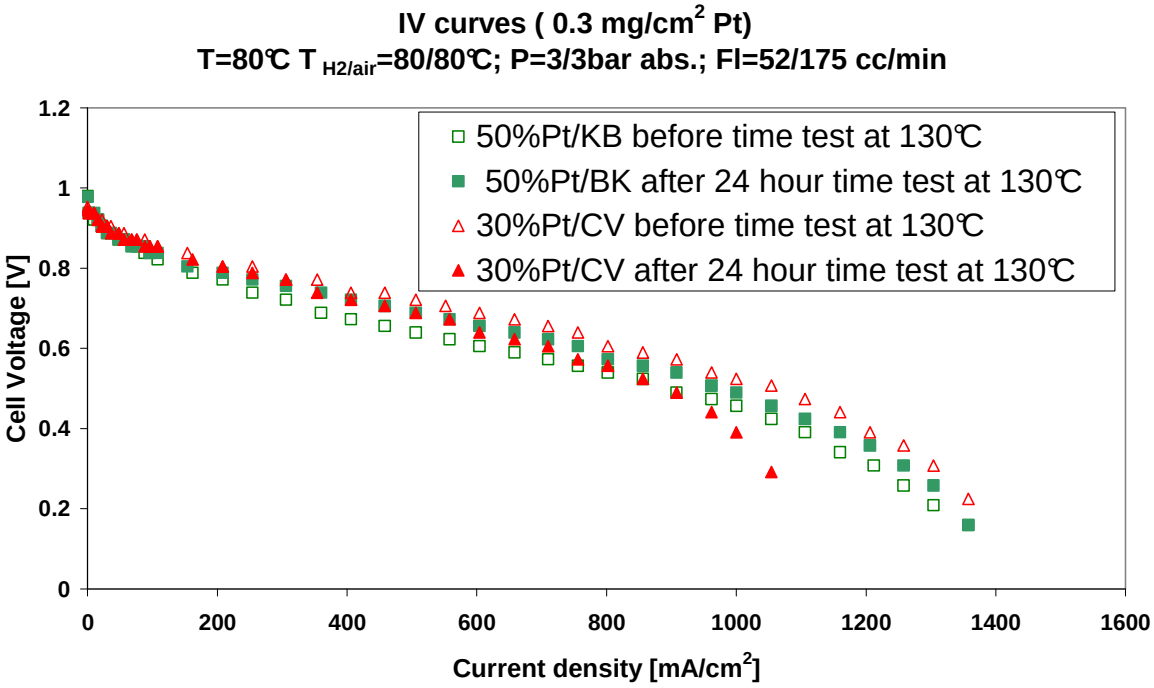

Figure 2.3: single cell IV curves comparison at 80°C: behaviour at start and end of endurance test at 130°C

Figure 2.4 shows that, despite the high maximum power value at the beginning of the time test at 130°C, the 30%Pt/CV MEA is strongly affected by high temperature degradation after coming back at 80°C as well. As visible, the power density decreased from 534.38 mW/cm² (with an OCV= 0.953V) down to 448.54 W/cm² (with an OCV= 0.945V).

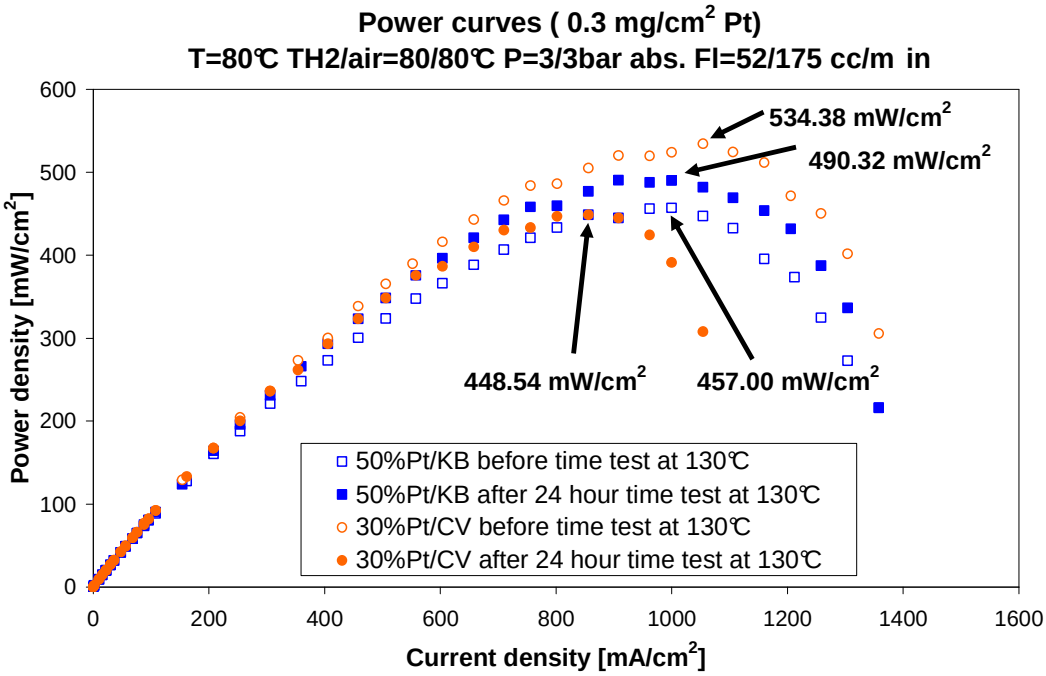

Figure 2.4: single cell power curves at 80°C, performance recorded at start and at end of endurance test at 130°C

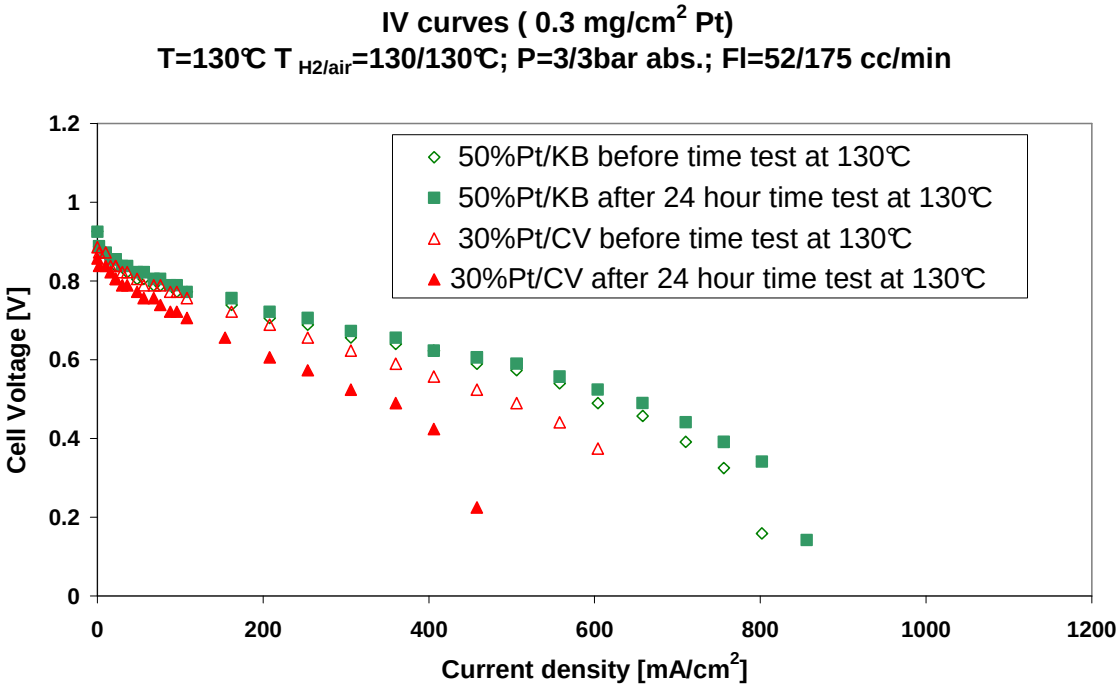

Figure 2.5: IV curves recorded at 130°C: different behaviours of the two preparations is shown (performance enhancement or degradation). OCV=0.886V for fresh 30%Pt/B, reduced to 0.857V after short endurance test. Stable OCV=0.925V was measured for 50%Pt/CV MEA.

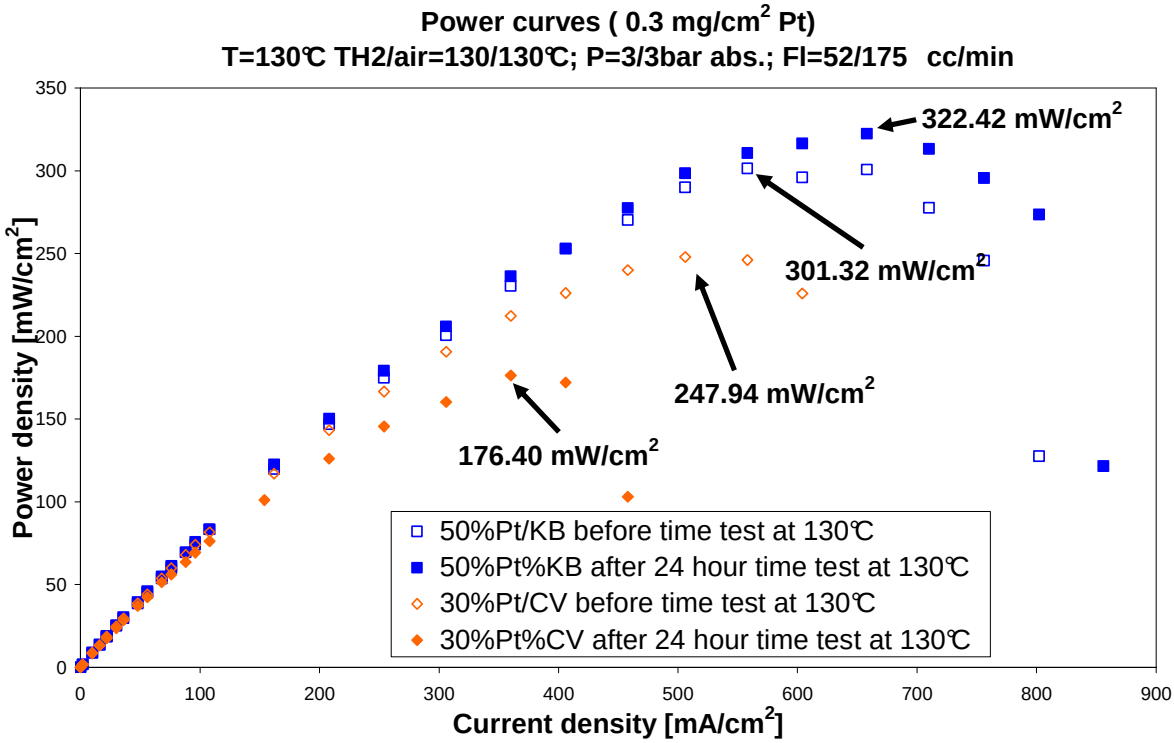

Figure 2.6: power performance at 130°C: 50%Pt/KB showed enhancement of performance. On the contrary 30%Pt/CV showed degradation.

By performing IV and power curves at 130°C as shown in **Figures 2.5 and 2.6**, the two preparations behaved differently each other. The former, 30%Pt/KB, reduced its performance after 24h time test at 130°C from 247.94 mW/cm² down to 176.40 mW/cm², moreover also a low OCV was noticed, and even 30mV reduction after time test (from 0.886V to 0.857V in **Figure 2.5**); on the contrary, the latter, 50%Pt/CV, increased the peak power after operation from 301.32 mW/cm² to 322.42 mW/cm² (the recorded OCV are 0.925V about identical in both measurements, in **Figure 2.5**).

2.5 - 1kW stack test

Polymer electrolyte fuel cell (PEMFC) technology for automotive applications requires operation at high working temperatures to improve efficiency, tolerance of contaminants and to enable simplification of the thermal and water management sub-systems. The operating conditions for the fuel cell stack targeted by the automakers are low pressure (P ≤ 1.5 bar abs.) and low relative humidity

(R.H. ≤ 25%). A high stack performance with suitable electrical efficiency (cell voltage ≥ 0.65 V) is desired over a wide temperature range from ambient temperature to about 110 -120 °C. Moreover, an easy and rapid startup, as well as the capability to sustain specific duty cycles, are pre-requisites for automotive applications.

In the last decade, considerable progress has been made on new polymer electrolyte materials for high temperature PEMFCs [1-4]. Several of these materials have shown interesting properties, but few efforts have been made to assess the new materials at a stack level. An investigation of performance and stability in a practical system, over a wide temperature range from ambient temperature to 130°C, is necessary for a full assessment of the PEMFC components and to clearly identify progress beyond the state-of-art.

Based respectively on the above described preparations two membrane-electrode assemblies (MEAs) were prepared by using a short side chain perfluorosulfonic membrane ("Aquivion", by Solvay-Solexis [5]).

This replaced the Nafion 115 membrane in single cell experiences since this was provided later during the framework of the project.

This study, in the frame of an Europen project (“Autobrane”), aims at validating the performance of the previously described MEAs in short stack configuration, by integrating them in a stack hardware, including end-plates, bipolar plates, macro-diffusion layers and gaskets, supplied by Nuvera.

The active area of each MEA was 360 cm^2. Each active cell was inserted in between two cooling cells. MEAs were assembled into short stacks of 5-6 cells connected in series and their electrochemical behaviour was investigated under different operating conditions as required for automotive applications.

2.5.1 - Test equipment and process conditions

The electrochemical tests were carried out at the CNR-ITAE by using an in-house made fuel cell stack test station. This included an hydraulic circuit mainly consisting of mass flow controllers, gas humidifiers, pre-heaters, water condensers and back-pressure valves. To control the stack temperature, a thermo-cryostat

apparatus was used (visible in **Figure 2.7 (a)**). A thermostating (cooling) fluid was passed through the cooling cells to maintain an almost constant temperature through the stack during polarization experiments. The actual stack temperature was measured by a thermocouple allocated inside the stack close to the outlet of the cooling fluid. Electrochemical polarizations were carried out by using a H&H 5600 electronic load.

Figure 2.7: Test stand equipment: (a) thermocryostat and sampling voltmeters, (b) digital memory oscilloscope for current interrupt measurements

The overall stack voltage and the voltages of the various cells were measured by Advanced Measurements high common mode rejection ratio digital voltmeters. All the instruments of the test station were controlled by a Labview® software and PXI National Instruments interface boards. The test station also included separate instrumentation for the electrochemical diagnostics i.e. a Gamry EIS300 electronic board for ac-impedance spectroscopy, an Agilent digital memory oscilloscope (shown in **Figure 2.7 (b)**) for the current interrupt method and a Powerten power supply for hydrogen pumping measurements.

2.5.2 - Performance measurements

Hydrogen and air stoichiometry values were 1.5 and 2, respectively, for currents larger than 72 A (a constant flow rate was used at lower currents), corresponding to a maximum value of 22 slpm of hydrogen and 72 slpm of air at 1A/cm^2. The temperature was varied in a wide range useful for automotive applications; ambient pressure (1 bar abs.) and a pressure of 1.5 bar abs. were

used. The relative humidity was controlled by varying the temperature of the humidifiers with respect to the operating temperature of the stack. The gas inlets were maintained at the same temperature of the humidifiers by heating tapes.

Polarization curves were recorded both at 80°C as a performance reference and up to 130°C, as done in single cell (for materials test). Moreover, low temperature tests were accomplished according to automotive test protocols.

Smaller activation losses at low current densities and ohmic losses at intermediate current densities were recorded with respect to conventional MEAs. The combination of highly active electrocatalysts with a thin (30 μm) short side chain perfluorosulfonic membrane with super-acid properties (equivalent weight equal to 790 g/eq.) allows to enhance the reaction rate at low temperatures. These properties are useful for a rapid start-up of the device.

The first stack (STACK1) was based on the MEAs containing 50%Pt/KB electrocatalyst showing less degradation in single cell. It was possible to reach operating temperature for the stack of 130°C. However the measured power decreased from 1.3kW to about 0.7kW in the range 80-130°C.

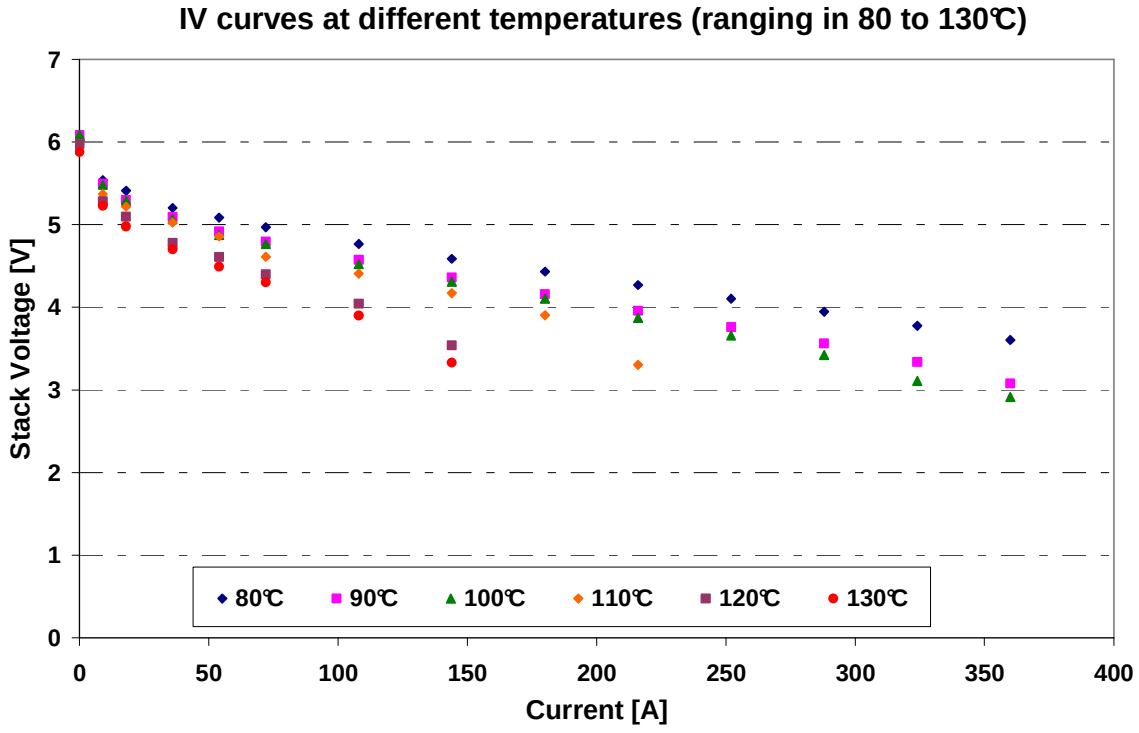

Figure 2.8: IV curves recorded for first stack and performance reduction in high temperature conditions (360 A corresponds to 1A/cm²)

Figure 2.8 shows IV curves related to tests performed at different temperatures. It is also shown that no significant voltage decay is recorded up to 100°C, over this threshold temperature, performance decreased so that it was not possible to drain high current to prevent the stack cells from the risk of inversion condition.

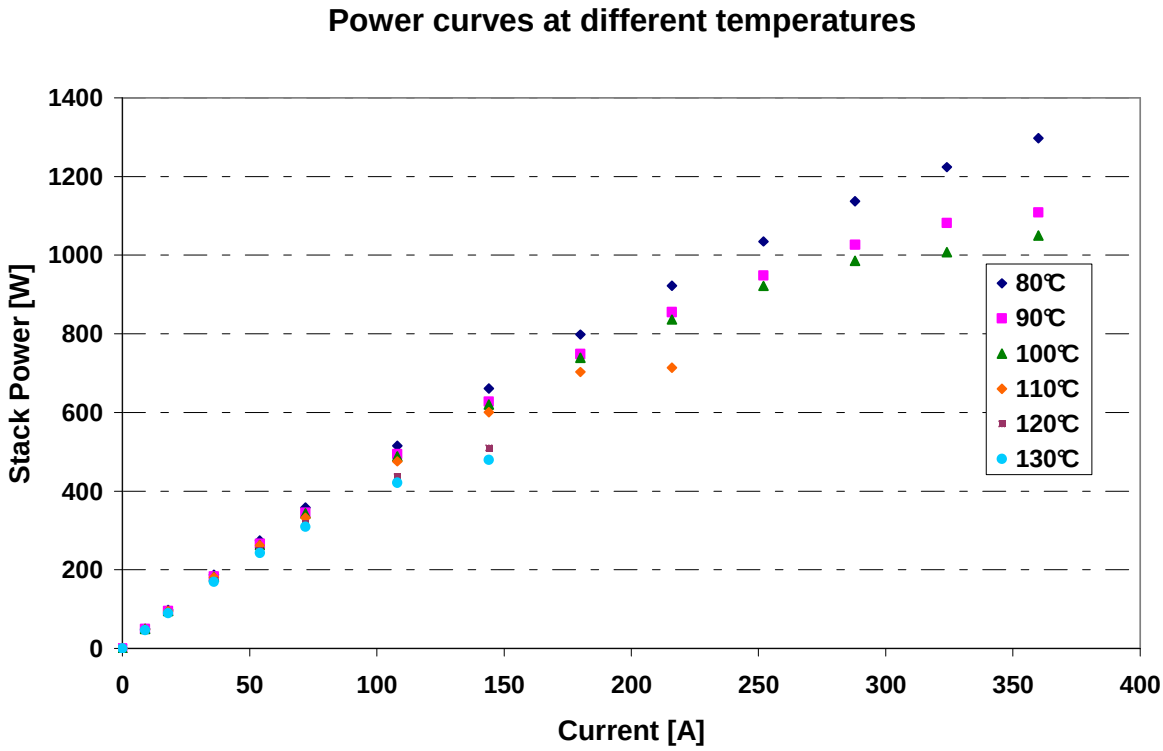

Figure 2.9: Power curves recorded for first stack at different temperatures (360 A corresponds to 1A/cm²)

As visible in **Figure 2.9**, the maximum power at different temperature had decrement while increasing temperature, in particular the stack reach 1kW of electrical power until temperature does not exceed 100°C. **Table 2.1** summarize the peak power recorded at each temperature.

Stack temperature [°C]	Stack peak power [W]
80	1296
90	1109
100	1055
110	717
120	511
130	481

Table 2.1: Peak power recorded at different temperatures and P=1bar abs

2.5.3 - Diagnostic procedures to improve stack performance

To investigate on the peak power reduction when temperature rises, current interrupt measurements were carried out. By means of a digital oscilloscope and the electronic load local control, current was abruptly zeroed (from a typical value of 180A, equivalent to 0.5A/cm^2), and the instantaneous voltage variation (to avoid relaxation phenomena induced by internal capacitances, the voltage behaviour is shown in **Figure 2.10** by an oscilloscope screen capture operation) was measured for each temperature.

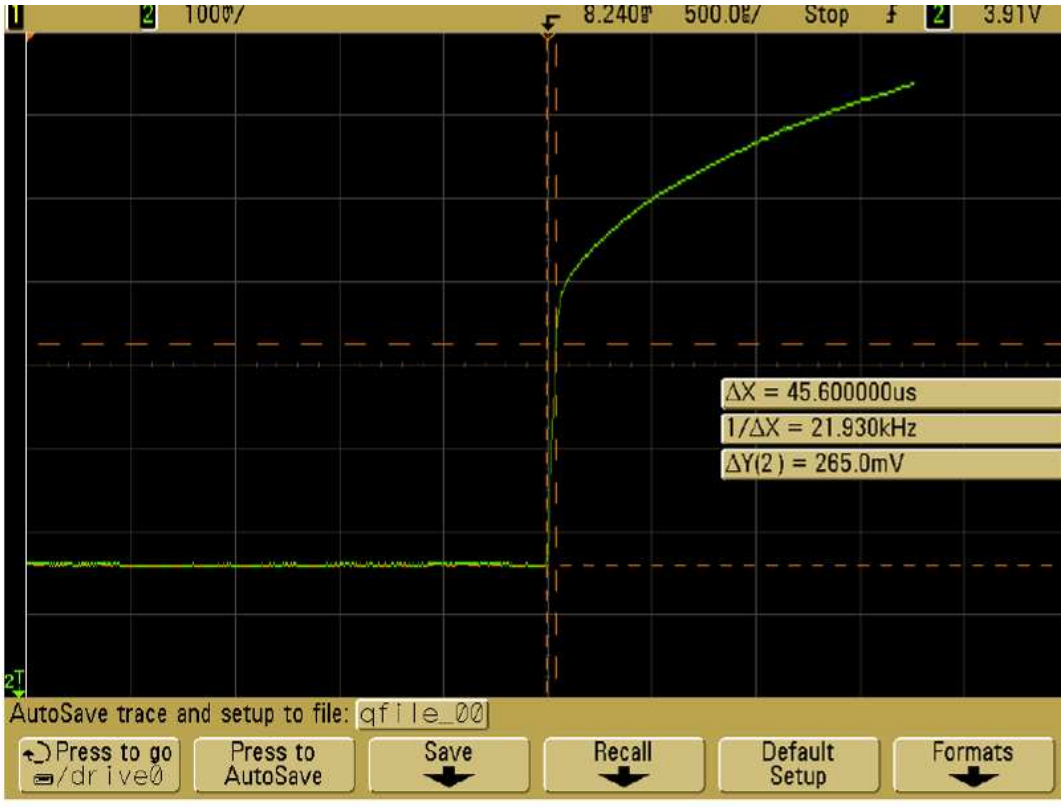

Figura 2.10:Current interrupt procedure: digital oscilloscope screenshot for measurement

The ratio between voltage and current variation is reported in **Figure 2.11** and represents the ohmic resistance of the stack. It appears clearly that the average resistance increase with temperature. This phenomenon limited the power available at the load input.

To have a deep insight of the stack behaviour, AC Impedance Spectroscopy technique was used. This technique allowed an estimation of the series and polarization resistances to individuate the rate determining step affecting the overall stack behaviour in the case of poor performance. An example of AC impedance spectra for the entire stack at different currents are reported in **Figure 2.11**. Measurements were accomplished in galvanostatic mode, by superposing a sinusoidal signal to a constant current level. To suppose a quasi-linearity of stack response, the chosen signal amplitude was levelled to 10% of the DC component.

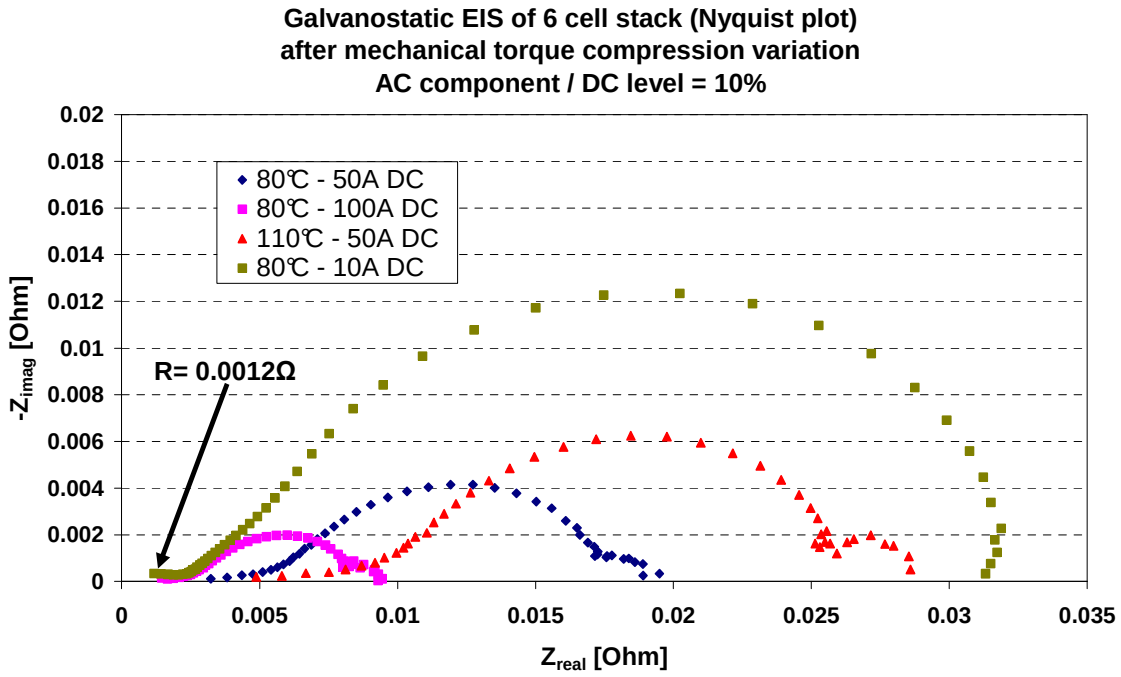

Figure 2.11: EIS diagram for 6 cell stack. After working at high temperature series resistance appears too high for the membrane composition. This evidence suggested to investigate the effects of high temperature operation on the stack compression. This was necessary to verify the correct tightness of the stack hardware after operating at high temperature.

The ohmic resistance measured at maximum frequency was in agreement with the value measured by current interrupt method.

As a verification of ohmic resistance measurement, the hydrogen pump method was applied to evaluate the resistance with a different procedure, at an intermediate value of the EIS temperature range, i.e. 90°C. The average value from two measurements (0.0028 Ohm, reported in **Figure 2.12**) is within the interval of the corresponding series resistance values (0.0012 @ 80°C, 0.0048 @ 110°C).

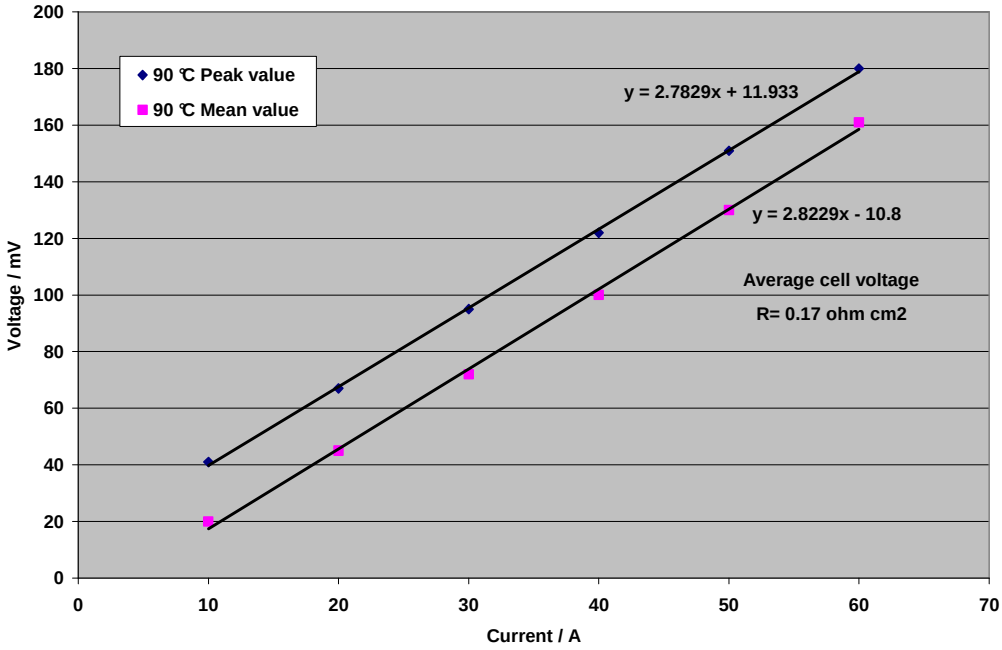

Figure 2.12: Hydrogen pump procedure results, the series resistance was averaged from two subsequent tests at 90°C. The equivalent specific resistance value is about 0.17 Ω * cm^2.

2.5.4 - Torque compression variation to improve contact resistance

A subsequent experiment to improve the stack performance was conducted by varying the mechanical compression on the cells. IV curves were recorded at three different compression torque value, and the results are reported in **Figure 2.13**.

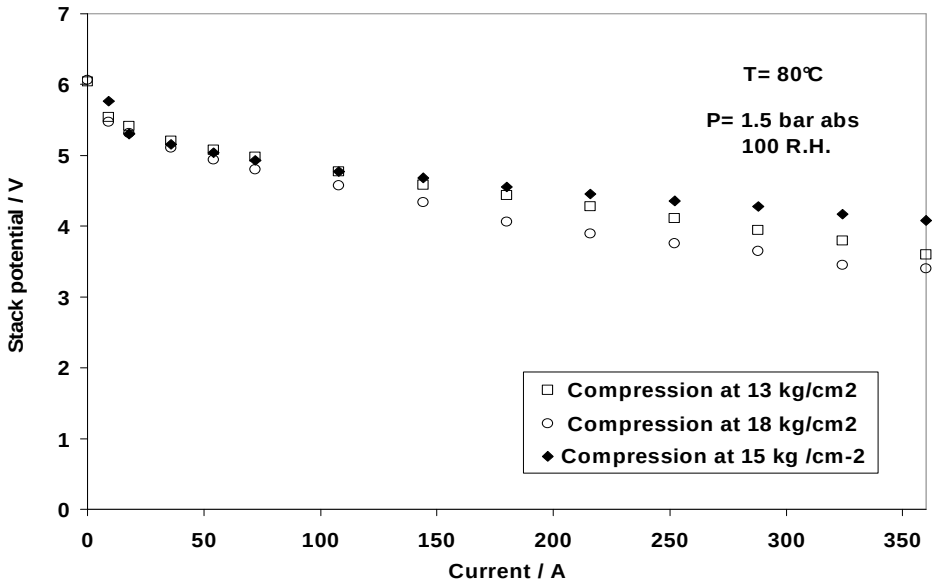

Figure 2.13: IV curves of 6 cell stack after varying the mechanical torque of compression rods. This was done in order to find a good compromise between contact resistance and gas flows constraints

As visible in **Figure 2.13**, a high compression allows to achieve lower contact resistance, but above a certain limit a large pressure drop was observed which caused an increase of mass transport constraints. It is also pointed out that an over-compression also caused the occurrence of MEAs damaging. The optimum value of compression is thus related to the MEAs characteristics as well as to the stack macroporous GDL/current collectors.

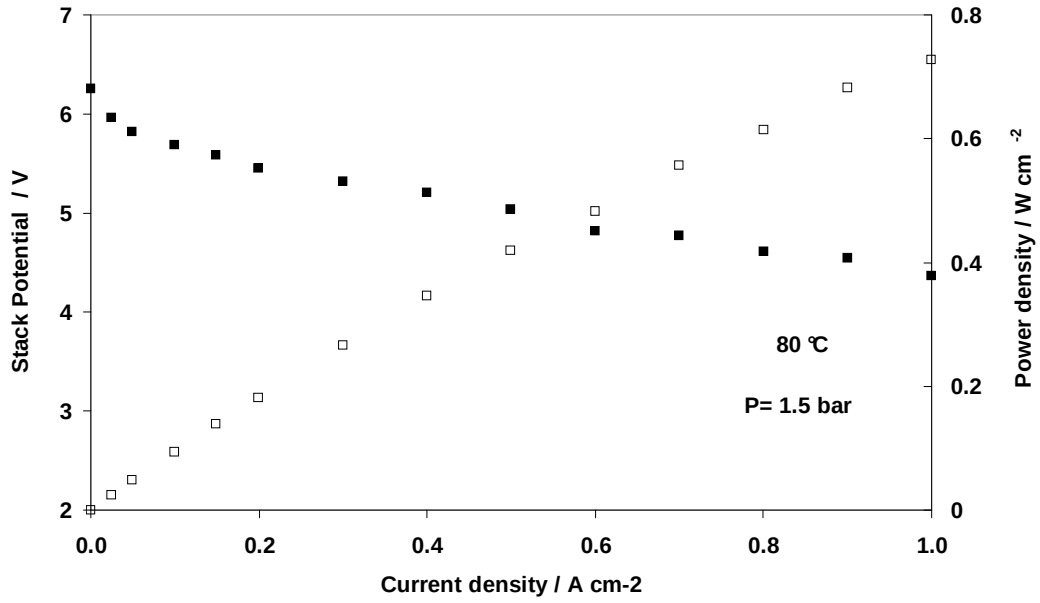

Figure 2.14: Polarization and power density curves at 80 °C of a single cell in Stack1. It was recorded with optimised working conditions, noticeable is the peak power density of 730mW/cm2.

Figure 2.15 shows two histograms related to the peak power in the high temperature range for two stacks assembled with six cells under different compressions. The effect of compression on the stack performance is also observed at the various temperatures. As reported above, the best performance of about 700 $mWcm^{-2}$ was achieved at 80 °C. The short stacks showed a suitable power output up to 100 °C with power densities exceeding 600 $mWcm^{-2}$ and a moderate decrease at slightly higher temperatures (110 °C). However, the performance decreased in the range 120-130 °C possibly due to dehydration effects as a consequence of the decrease of relative humidity as indicated in **Figure 2.15**.

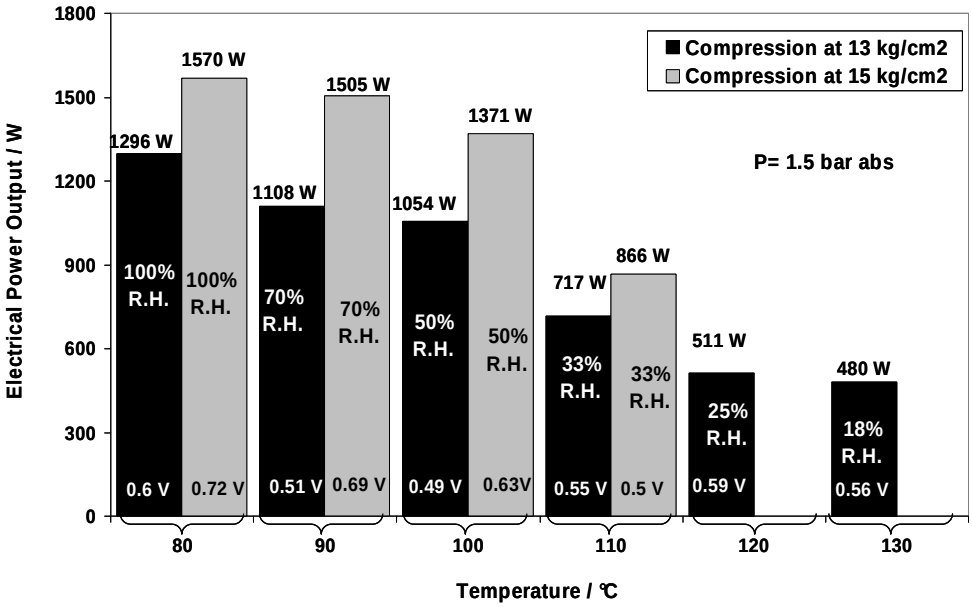

Figure 2.15: Maximum power achieved at different temperature (comparison of results obtained by varying the compression torque).

The best performance was achieved at 80 °C with a peak power density of about 700 mW cm-2 (R.H.A. 100%, R.H.C. 50%, Air stoich. 2, H2 stoich. 1.5) in the presence of an optimised stack compression. Typical cell resistances of 0.05 -0.08 Ohm cm2 were measured at 80 °C under optimal compression whereas these reached the values of 0.15-0.18 Ohm cm^2 under poor compression (as visible in **Figure 2.11** and **Figure 2.12**). These results were confirmed by cross-comparison of the data obtained from the current interrupt, ac-impedance spectroscopy and hydrogen pumping methods.

The cell resistance increased from 0.05 to about 0.2 Ohm cm2 on increasing temperature from 80 °C to 110 °C, due to the membrane dehydration.

2.5.5 - Second short stack test

The second stack (STACK2) consisted of MEAs based on the Pt/CV catalyst. In this case the maximum temperature reached was 110°C. At higher temperature significant degradation was observed during operation with decrease of OCV. The stack test was interrupted to avoid recombination of the H_2 and O_2 in the membrane electrolyte catalyst by Pt dissolution.

The second short stack was also tested to envisage the differences from the first one when operated up to 110°C. Also for this stack, the H_2 and air flows were regulated at, respectively, 1.5 and 2 times the stoichiometric value, for each current value.

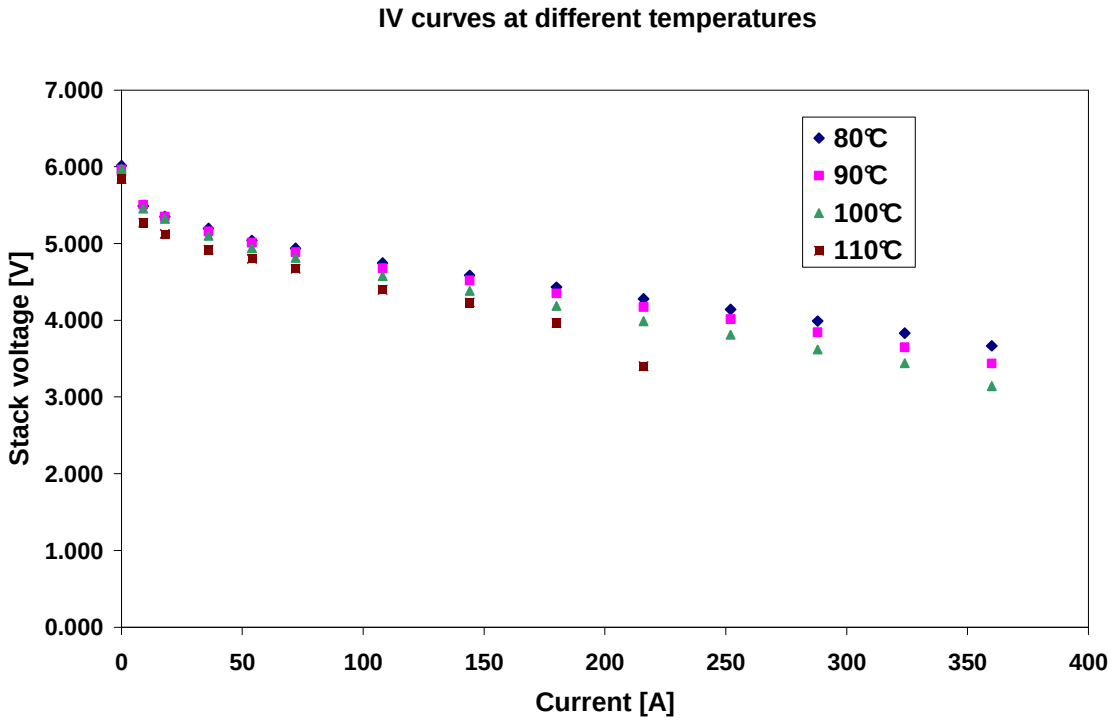

Figure 2.16: IV curves for second short stack at different temperatures in the range 80 to 110°C

The IV curves were recorded and reported in **Figure 2.16**. Those plots indicate that the voltage available for an electrical load decreased as the stack temperature reached 110°C whereas no more than slight differences are verified for lower temperatures.

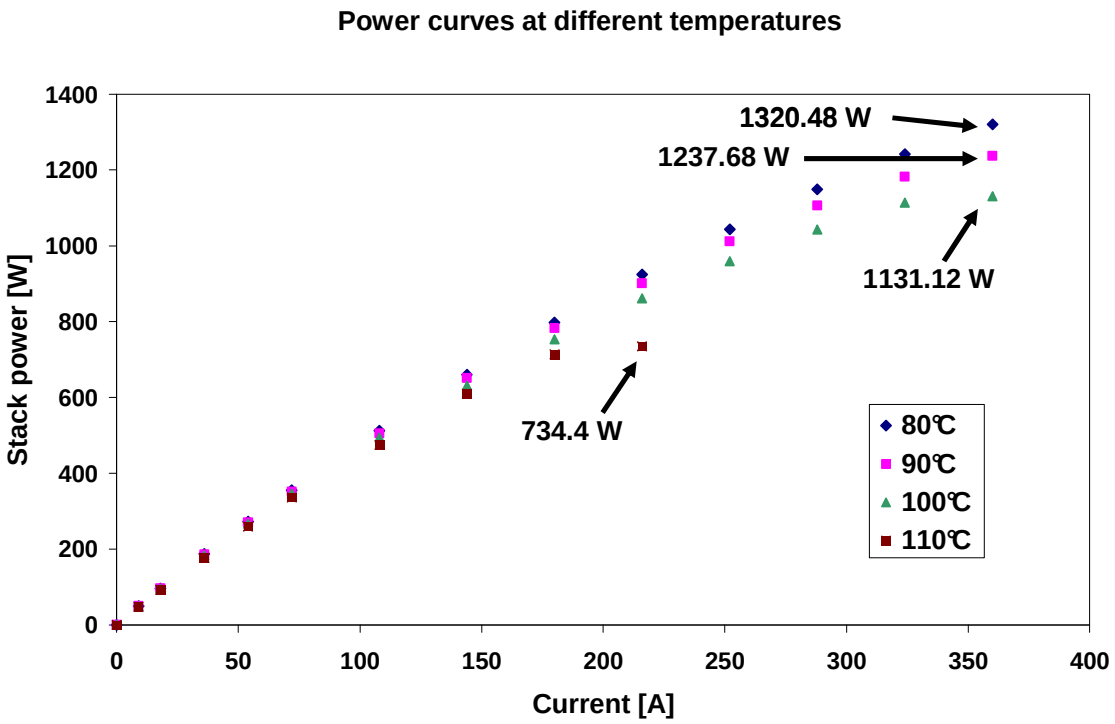

Figure 2.17: Power curves for second stack tested. The dramatic performance reduction over 110°C

The corresponding power curves, reported in **Figure 2.17**, indicate a deep decrease of performance at 110°C, from 862W at 100°C down to 734W at 110°C at the same current load 216A (corresponding to a 15% reduction at 0.6 A/cm^2).

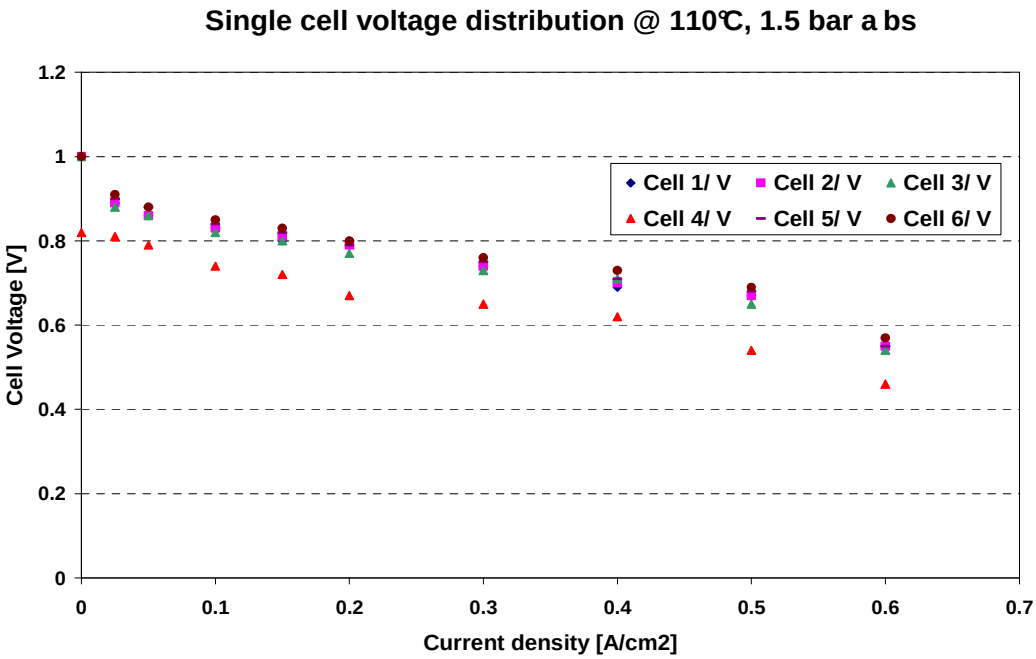

Figure 2.18: Single cell voltages measured to discover the cause of performance decrement at 110°C

With the purpose of understanding the main cause of performance reduction at high temperature, the single cell IV curves were recorded. As shown in **Figure 2.18**, it is clear that only one cell (cell #4) is strongly affected by temperature effects.

Moreover, the voltage loss appears at 0A (OCV condition) as well. For this reason, the cell seems to be affected by hydrogen crossover. The crossover hypothesis was verified thanks to the hydrogen pumping technique, with this purpose cell #4 was compared with a regularly working cell (cell #6 in the test) by feeding the stack with hydrogen at the anode and nitrogen at the cathode; a 400mV potential was imposed by means of a linear power supplier and the circulating current was measured. The recorded values (reported in **Figure 2.19** as a 19A current) indicated a hydrogen flow (typical crossover behaviour) through cell #4, on the contrary any current was not measured when the same potential was imposed on cell #6.

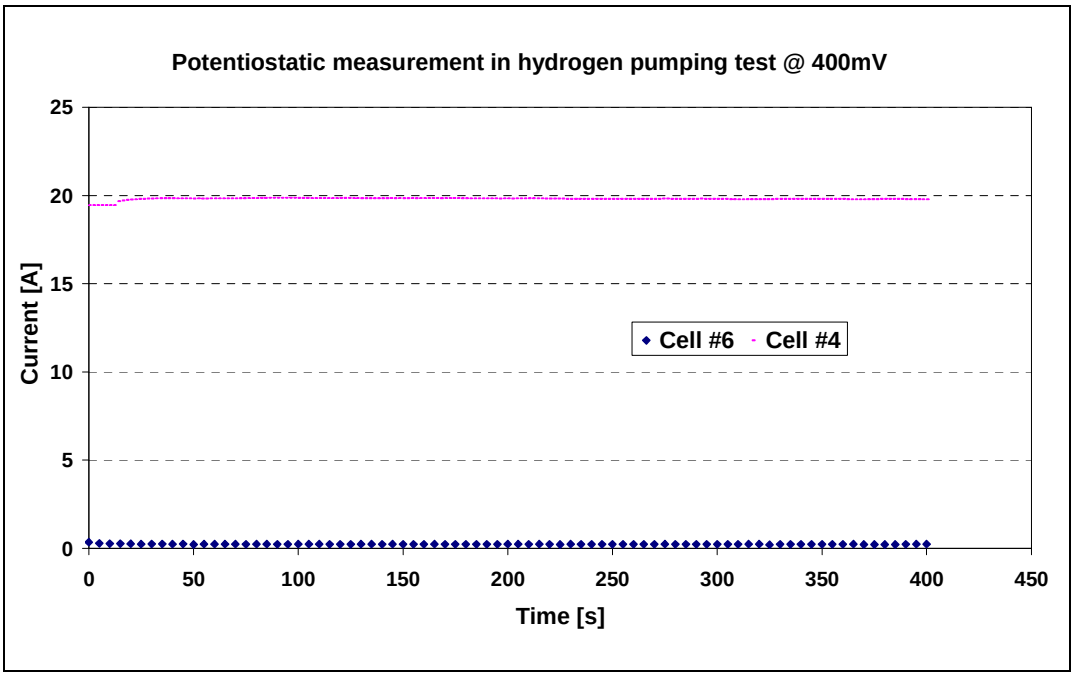

Figure 2.19: hydrogen crossover measurement applied on a working cell (Cell#6)and a damaged cell (Cell#4). The high current flow needed to set a 400mV potential on cell#4 shows the behaviour of hydrogen crossover phenomenon.

A slight increase of performance is registered at 80 °C when the pressure is increased from 1 to 1.5 bar abs. at 100 % R.H, as visible in **Figure 2.20**. This means that an increase of pressure is especially useful at temperatures above 100 °C to maintain a small amount of liquid water inside the membrane; however, it can not exceed a certain limit which is determined by the technology of the air blowers for automotive applications presently available on the market. An air compressor is generally excluded from the automotive applications because of the high electrical power consumption and the large space needed by this device on board relative to the blower.

The slight increase of performance with the pressure under fully humidified conditions at a conventional operating temperature is mainly due to the increase of oxygen solubility at the electrode-electrolyte interface that enhances mass transport properties. Furthermore, a small enhancement in the activation-controlled region is also determined by the positive reaction order (~1) with respect to the oxygen concentration for the oxygen reduction process in acidic electrolytes.

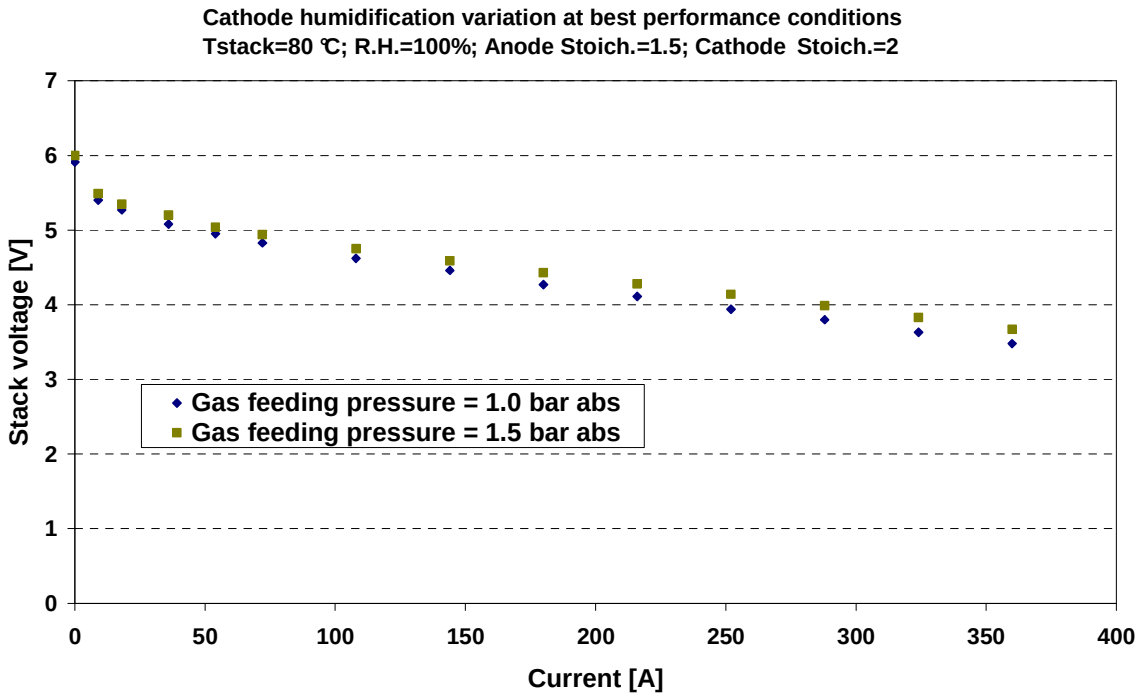

Figure 2.20: Variation in gas feeding pressure from 1.0 to 1.5 bar abs. to measure performance enhancement reachable in better working conditions

After this test, a second working condition variation (with respect to the optimal conditions discovered so far, i.e. stack temperature at 80°C and outlet pressure at 1.5 bar abs), for this stack, was the change of gas humidification at the cathode form 100% to 50% to find the possible loss of performance in suboptimal working conditions.

The higher recorded voltage (and power) for 50% cathode relative humidification at conventional temperature is attributable to a lower flooding effect.

A further increase in performance at high current densities was achieved at 80 °C and 1.5 bar abs. by decreasing the temperature of the cathode humidifier from 80 °C to 64 °C. The corresponding variation of relative humidity at the cathode is from 100% to 50% R.H. (**Figure 2.21**).

The choice of this new set point is explained now.

The gas humidification control mechanism is based on the saturation temperature of the gas with water. The bubblers, full of distilled water, was supplied with gases (one for fuel, one for oxidant) from the bottom; the bubblers

included sponge shaped distributors to spread the gas through the water. When the gases reach the top of the water column, they drag some water, whose percentage content depends on the water temperature.

The numerical expressions used to evaluate the steam content, by means of the relative humidity (RH, defined as the ratio between the actual absolute humidity value in the gas and the maximum water steam content at a given temperature) are reported as follows:

$$E_s = 6.11*10^{\frac{7.5*T_c}{237.7+T_c}}$$

$$E = 6.11*10^{\frac{7.5*T_{dc}}{237.7+T_{dc}}}$$

$$RH = \frac{E}{E_s}100\%$$

Provided that the whole process happened at atmospheric pressure, that equation is based on the relations that are between "vapour pressure" and the corresponding gas temperature both in saturation condition. E is the "vapour pressure", E_s is "saturation vapour pressure", T_c is the gas temperature in Celsius degrees, T_{dc} is the dewpoint temperature (usually, the gas temperature is referred as "dry bulb temperature", and the water temperature as the "wet bulb temperature"). The dewpoint is defined as the temperature at which (for a fixed pressure value) a water/air mixture is saturated with water steam, and every extra water steam content, if added, is converted into liquid water. In these conditions, the gas flow that goes through the bubbler will drag a unique amount of water.

So, by replacing the literal expressions with the numerical values (Tc= 80°C as per the applied test protocol procedure, with cathode air flow, and RH=0.5), were calculated:

$$E_s = 6.11*10^{\frac{7.5*T_c}{237.7+T_c}} = 6.11*10^{\frac{7.5*80}{237.7+80}} = 477.29\,mbar$$

$$E = RH * E_s = 0.5*477.29 = 238.65\,mbar$$

$$T_{dc} = \frac{237.7 * \log\left(\frac{E}{6.11}\right)}{7.5 - 237.7 * \log\left(\frac{E}{6.11}\right)} = \frac{237.7 * \log\left(\frac{238.65}{6.11}\right)}{7.5 - \log\left(\frac{238.65}{6.11}\right)} =$$

$$= \frac{377.36}{5.91} = 63.8°C \approx 64°C.$$

Hence, in order to impose a RH value of 50% in the cathode stream, it is necessary to set the water temperature to 64°C into the bubbler.

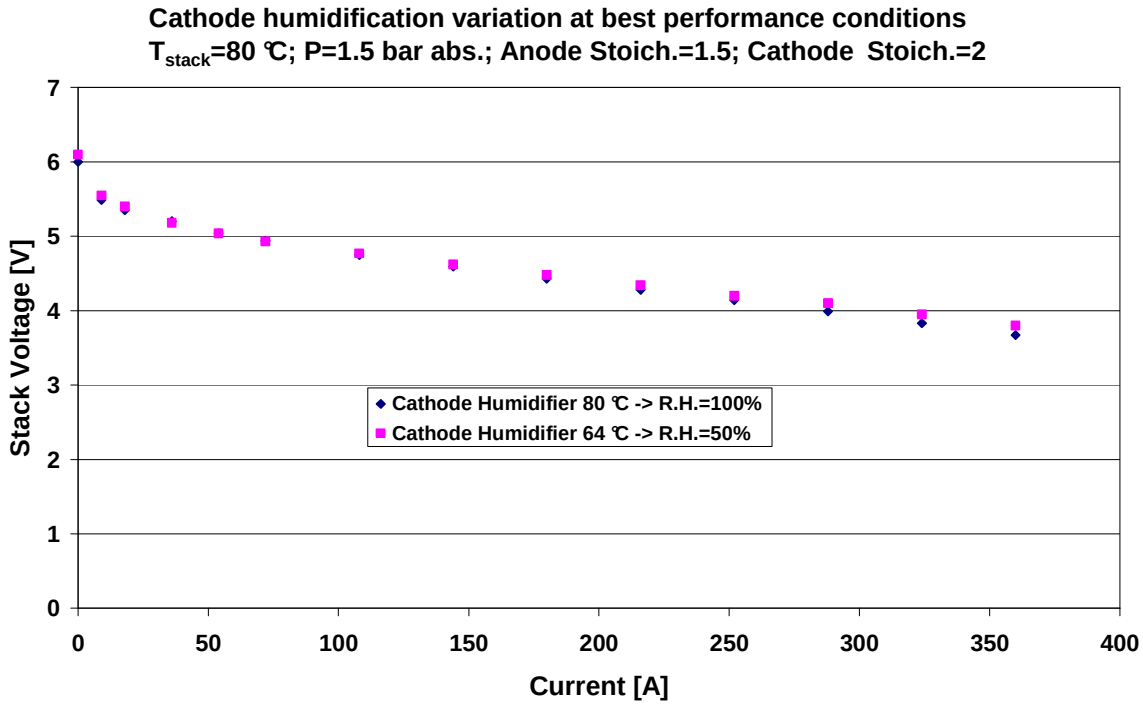

Figure 2.21: Cathode humidification variation test to approach automotive sector requirements. The better values recorded at 50% cathodic RH

The recorded power densities under these conditions were in the range of 600-700mW/cm^2 at an average cell voltage of 0.6-0.65 V (**Figure 2.22**). These results appear appropriate both in terms of performance and electrical efficiency for automotive applications. The cell voltage distribution for the various cells in the stack was sufficiently homogeneous (**Figure 2.22**) indicating suitable mass transport properties for MEAs and stack hardware design.

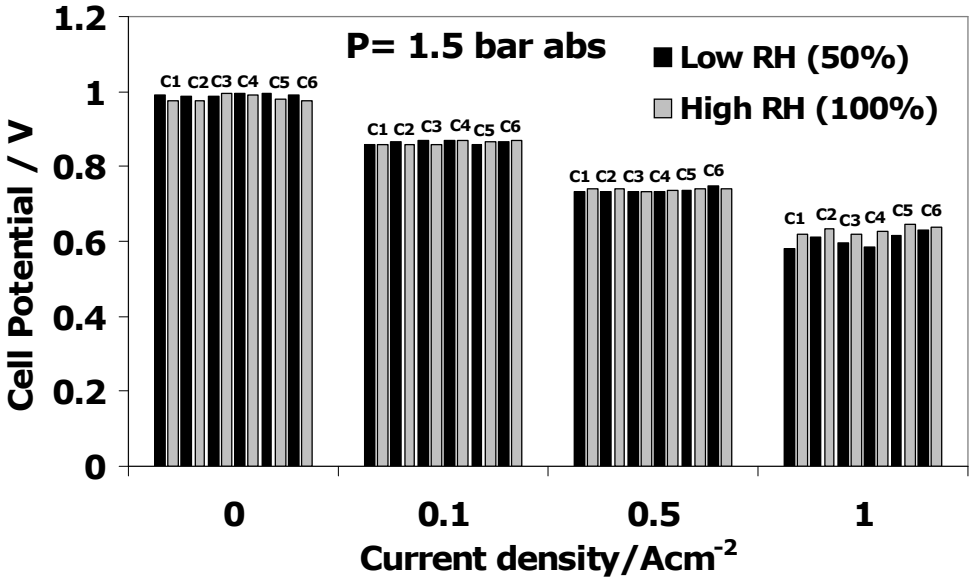

Figure 2.22: Cell voltage distribution while operating at two different cathodic RH contents. The voltage distribution appeared homogeneous for each pair of working conditions (RH - current density)

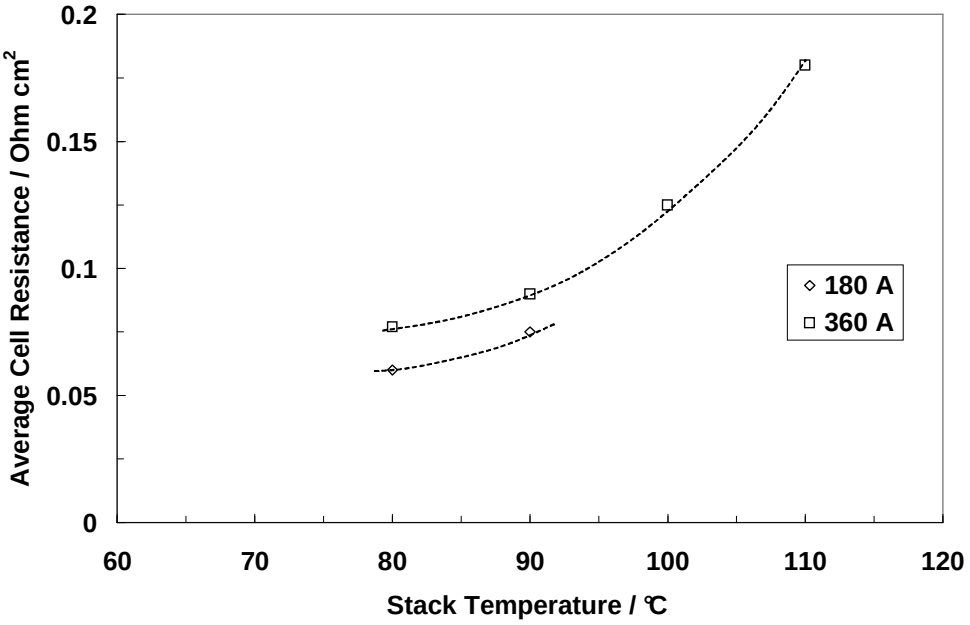

Figure 2.23: comparison of ohmic resistance at different operating current interrupt for different temperature. Measurements at temperatures higher than 90°C at 360A were not carried out due to the instability temperature management of the stack.

As done in the study of the first stack, current interrupt method was applied to highlight the series resistance variation while increasing temperature. The results are reported in **Figure 2.23**, they showed an increase with the temperature,

above 80 °C, related to dehydration and a decrease with the operating current due to the occurrence of internal humidification.

Although the Aquivion membrane showed significantly better water retention properties at high temperature than the conventional perfluorosulfonic membrane, the most effective proton conduction mechanism still relies on the so-called vehicle mechanism where proton transport is assisted by water molecules. At high temperature, a Grotthus mechanism may also contribute to the overall conductivity and the thin (30 µm) Aquivion membranes also favour the back-diffusion to the anode of the water produced at the cathode. Stack operation at high current densities is thus essential to promote the internal self-humidification of the MEAs. Typical polarization and power density curves for a cell in a short stack at 110 °C, 1.5 bar abs., 33% R.H. in the presence of mild stack compression is shown in **Figure 2.24**. A power density of about 370 mW cm^{-2} was recorded at a cell voltage of 0.6 V. These polarization results are promising for the automotive applications, however, it should be pointed out that polarization experiments were performed under well controlled temperature conditions i.e. the stack reached the thermal equilibrium at the operating current density.

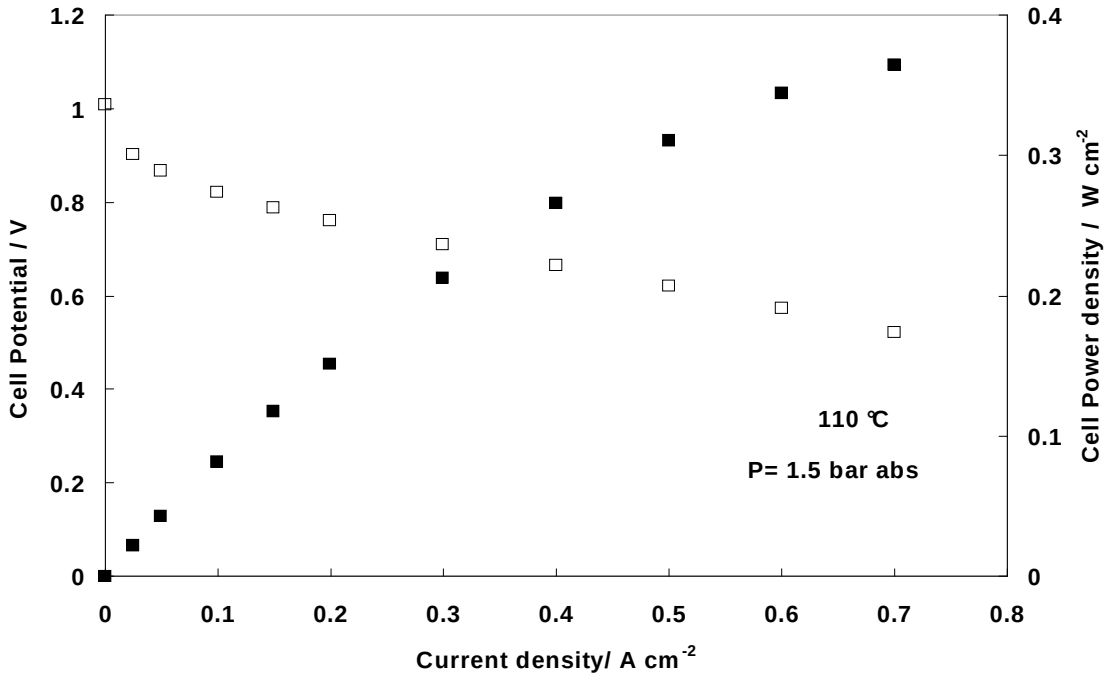

Figure 2.24: Polarization and power density curve at 110 °C and 33% R.H. of a single cell in STACK2

2.5.6 - Duty cycle test

Under practical operation conditions under automotive applications, the stack may experience rapid changes of current at both conventional and high working temperatures.

Simplified duty cycles of current and temperature were thus applied to the stack and the corresponding variation of the stack voltage and actual temperature was monitored. The initial and final of several consecutive duty cycles are shown in **Figure 2.25**. The initial stack compression was 10 kg cm^{-2} in this case. Although some voltage/temperature fluctuation was observed, no significant decay of performance was recorded after these cycles; the temperature deviation with respect to the set-point of the cooling device was slightly larger than that observed in polarization experiments; however, the recorded stack voltage was similar to that observed in the polarization current for similar operating conditions and stack compression.

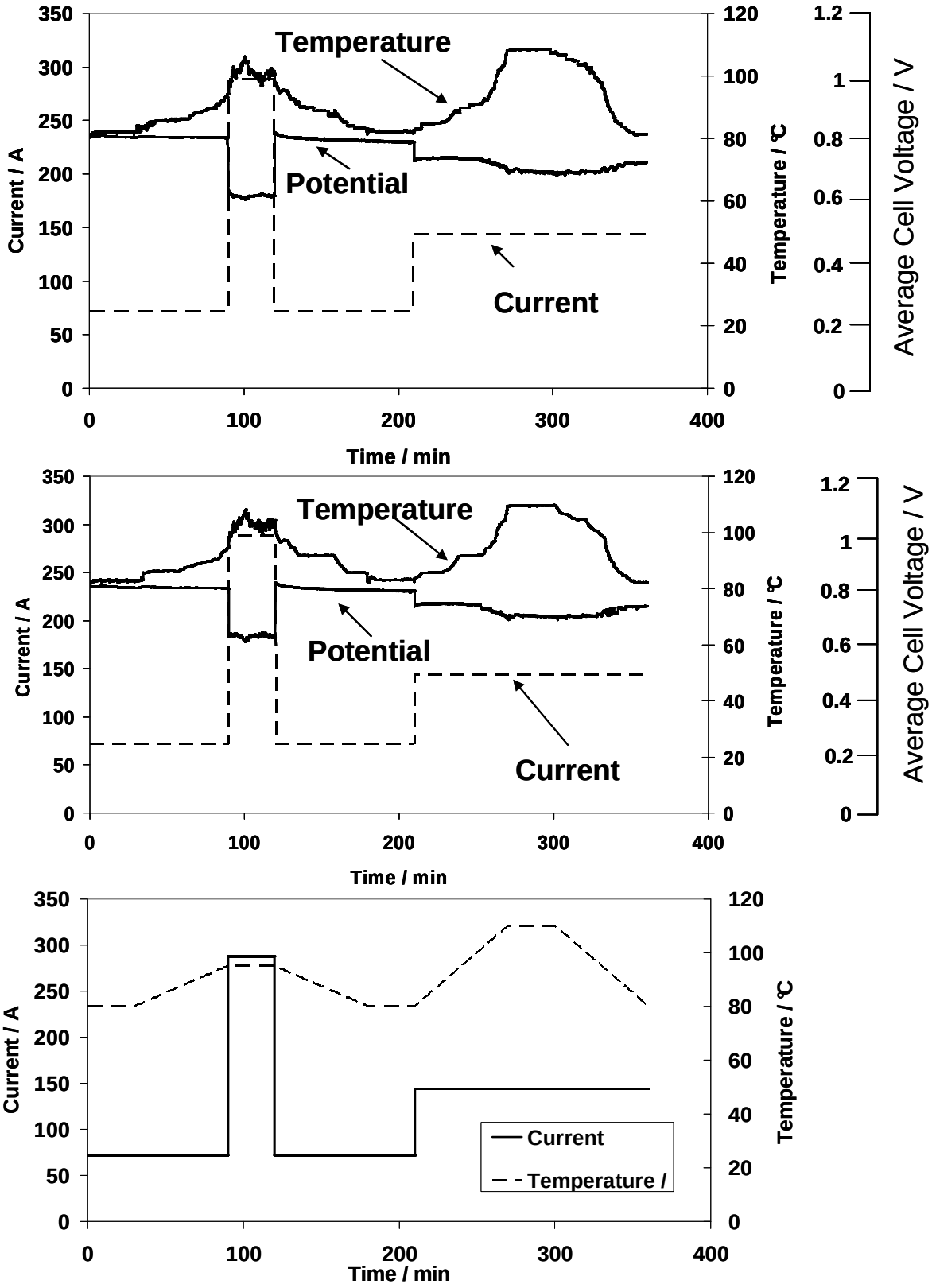

Figure 2.24: Duty cycles (top: initial; bottom final) with nominal temperature set point of the cooling apparatus. (STACK2 - active area 360 cm2).

2.5.7 - Conclusions

The stacks showed appropriate performance in a wide temperature range from room temperature to 100 °C. At 110 °C and 1.5 bar abs., a moderate decrease of performance was observed for STACK1 and an irreversible increase of ohmic resistance for STACK2. During these operations [6], MEAs hydration in the stack at high temperature was mainly assured by the internal humidification and the back-diffusion of the water from the cathode to the anode through the thin (30 µm) MEAs.

Power densities of about 370-400 mW cm^{-2} were recorded at 110°C (Air stoich. 2, H_2 stoich. 1.5 and 1.5 bar abs.). These polarization results are promising for the automotive applications even if quite far from the performance achieved at 80°C i.e. 700mW/cm^2.

Moreover, an important factor affecting stack performance is the compression torque, that must be evaluated and optimized in order to have a compromise between contact (ohmic) resistance and reduction of performance due to the increase of mass transport constraints and even possible cell damage.

Typical cell resistances of 0.05 - 0.08 Ohm cm^2 were measured at 80 °C under optimal compression whereas the resistance reached the values of 0.15 to 0.29 Ohm cm^2 under poor compression for STACK1.

On the contrary, STACK2 showed a strong degradation of performance while operated at high temperature, especially above 110°C, in agreement with the behaviour of single cell results. It appears that the single cell analyses can provide useful insights on catalyst and MEA stability in the stack. The better resistance to degradation of the Ketjen Black based catalyst may be attributed to the high surface graphiticity index of this material and to the proper metal support interaction that compensate for the high surface area.

2.5.8 - References

[1] J. Wang, S. Wasmus and R. F. Savinell, J. Electrochem. Soc. 142, 4218 (1995).

[2] A. S. Aricò, P. Creti, P. L. Antonucci and V. Antonucci Electrochem. Solid-State Lett. 1, 66 (1998) .

[3] K. D. Kreuer J. Membr. Sci. 185, 29 (2001).

[4] L. Tchicaya-Bouckary, D. J. Jones and J. Rozière, Fuel Cells 1, 40 (2002).

[5] V. Arcella, C. Troglia, and A. Ghielmi, Ind. Eng. Chem. Res. 44, 7646 (2005).

[6] A. S. Aricò, A. Di Blasi, G. Brunaccini, F. Sergi, V. Antonucci, P. Asher, S. Buche, D. Fongalland, G. A. Hards, J. D. B. Sharman, A. Bayer, G. Heinz, R. Zuber, M. Gebert, M. Corasaniti, A. Ghielmi, D. J. Jones. - ECS Transactions, 25 (1) 1999-2007 (2009) 10.1149/1.3210756 © - The Electrochemical Society.

Conclusions

Similar performances in terms of rated power density were achieved for 1kW HT-PEMFC and IT-SOFC devices as compared to small single cell tests. They showed suitable behaviour under real application conditions.

Both technologies successfully worked in an extended temperature range, with respect to the state of art, confirming the possibility of scaling up the results achieved in single cells even to relevant size devices.

Concerning with the mass production of complete systems, there are issues common to both technology:

- the humidification system: in SOFC devices for operation in natural gas, despite not being necessary, the steam reforming gives higher conversion efficiency than dry reforming; in PEFC devices it was noticed that new membranes have good performance even if RH decreases down to less than 50% in a wide temperature range (80-110°C);
- the compression mechanism: to assure absence of leakage through the border of large area planar cells and to achieved a good ohmic contact for contiguous electrodes (so that ohmic resistance is low).

Moreover, the stacks showed good voltage stability at the nominal working conditions, in particular PEMFC stacks demonstrated good resistance in simplified duty cycle, and the SOFC stack achieved optimal performance even after a thermal cycle.

For this reason, according with the targeted applications, the stacks can be exploited in power production and they let envisage significant cost reduction in the next future for fuel cell technology.

Future works, in order to enhance performance of a prototype system, will involve co-generation application for SOFC stacks, in terms of coupling with heat exchanger, reversible heat pumps or energy storage devices (to improve both pump efficiency and energy saving). This should give guidelines to the design of market ready hybrid systems.

List of publications

1) A. S. Aricò, A. Di Blasi, G. Brunaccini, F. Sergi, V. Antonucci, P. Asher, S. Buche, D. Fongalland, G. A. Hards, J. D. B. Sharman, A. Bayer, G. Heinz, R. Zuber, M. Gebert, M. Corasaniti, A. Ghielmi, D. J. Jones. **High temperature operation of a solid polymer electrolyte fuel cell stack based on a new ionomer membrane**. ECS Transactions, 25 (1) 1999-2007 (2009) 10.1149/1.3210756 © - The Electrochemical Society

2) Andaloro, L., Ferraro, M., Brunaccini, G., Sergi, F., Antonucci, V. **From distributed generation to smart grids: Integration of H2 and renewable energy towards zero emissions home**. (2009) ECS Transactions, 17 (1), pp. 673-684.

3) Ferraro, M., Sergi, F., Brunaccini, G., Dispenza, G., Andaloro, L., Briguglio, N., Antonucci, V. **PEM fuel cell systems for distributed energy: Actual performance, lifetime and reliability of a pure hydrogen pre-commercial system**. (2009) ECS Transactions, 17 (1), pp. 233-239.

4) Chávez-Ramírez, A.U., Muñoz-Guerrero, R., Durón-Torres, S.M., Ferraro, M., Brunaccini, G., Sergi, F., Antonucci, V., Arriaga, L.G. **High power fuel cell simulator based on artificial neural network**. (2009) International Journal of Hydrogen Energy, . Article in Press.

5) Ferraro, M., Sergi, F., Brunaccini, G., Dispenza, G., Andaloro, L., Antonucci, V. **Demonstration and development of a polymer electrolyte fuel cell system for residential use**. (2009) Journal of Power Sources, 193 (1), pp. 342-348.

6) Brunaccini, G., Lo Faro, M., La Rosa, D., Antonucci, V., Aricò, A.S. **Investigation of composite Ni-doped perovskite anode catalyst for electrooxidation of hydrogen in solid oxide fuel cell**. (2008) International Journal of Hydrogen Energy, 33 (12), pp. 3150-3152.

7) Ferraro, M., Sergi, F., Cretì, P., Brunaccini, G., Andaloro, L., Antonucci, V. **Direct hydrogen 5.0 kW PEM fuel cell system supplying an uninterruptible power supply** (2007) ECS Transactions, 5 (1), pp. 791-801.

Acknowledgements

I would like to thank some people that have been fundamental for my research activity carried out at CNR-ITAE.

First of all, I would like to remember the contribution of Dr. Antonino Aricò and Dr. Vincenzo Antonucci and their constant availability every time I asked them for suggestion both for working and personal life.

But this work would not have been carried out without the help of my colleagues that I like mentioning here without distinction, as a single and unique working group: Laura Andaloro, Nicola Briguglio, Alessandra Di Blasi, Giorgio Dispenza, Marco Ferraro, Massimiliano Lo Faro, Giuseppe Napoli, Francesco Sergi, Stefania Siracusano, and Alessandro Stassi. Everyone has contributed in a different way to allow me to acquire a significant research experience during these last five years.

At the end, last thought is for my dear family for every single moment spent together and for their continuous support to me.